
# BOUNDARY LAYER PREDICTION IN A COMPRESSOR CASCADE

A DISSERTATION SUBMITTED
IN PARTIAL FULFILMENT OF THE REQUIREMENT
FOR THE AWARD OF THE DEGREE OF

**MASTER OF SCIENCE (ENGINEERING)**

IN

MECHANICAL ENGINEERING (HEAT POWER)

BY

**IZHARUL ISLAM**

**DEPARTMENT OF MECHANICAL ENGINEERING**
**ZAKIR HUSAIN COLLEGE OF ENGG. & TECH.**
**ALIGARH MUSLIM UNIVERSITY**
**ALIGARH**

MAY, 1980

CERTIFICATE

This is to certify that the dissertation entitled "Boundary Layer Prediction in a Compressor Cascade" is being submitted by Mr. Izharul Islam in partial fulfilment of the requirements for the award of degree of Master of Science in Mechanical Engineering (Heat Power). This work has been carried out under my supervision and guidance and is not submitted anywhere, to the best of my knowledge, for the award of any degree or diploma.

ALIGARH:
Dated: 30/5/87

(Dr. Ghulam Abdul Quadir)
Supervisor
Reader of Mech. Engg.
Z.H.College of Engg. & Tech.
A.M.U.Aligarh.

ACKNOWLEDGEMENT

I am greatly indebted to Dr. Ghulam Abdul Quadir, Reader, Mechanical Engineering Department, for his kind guidance and devotion of his valuable time for me in carrying out this dissertation work.

I am thankful to Prof. J.A.Munir, Head of the Mechanical Engineering Department, for providing the necessary facilities.

I am also thankful to Dr. Noor Afzal, Professor, Mechanical Engineering Department, for his encouragement during the work.

( IZHARUL ISLAM )

ALIGARH.
Dated: 30/5/80

## C O N T E N T S

ABSTRACT

The growth of boundary layer on the blades of compressor cascades has been studied. Transition points on the blade surfaces were predicted using the well-known Michel's method. It is observed that the above method failed to predict the transition point on the blade pressure surface for $10^{o}$ incidence at lower Reynolds numbers. Some other method may, therefore, be used to predict the transition point under the above circumstances. The value of H at transition is assumed to be equal to 1.4 in all calculations. Thwaites' method and Truckenbrodt's method are usedd to calculate the laminar and turbulent boundary layer growth respectively Final results are presented in the form of $C_D$ versus Reynolds numbers as suggested by Speidel & Scholz.

## NOMENCLATURE

| | |
|---|---|
| $u$ , $v$ | Components of velocity in boundary layer over the blade. |
| $U$ | Potential flow velocity. |
| $U_1$ , $U_2$ | Potential flow velocities at inlet and exit of the cascade. |
| $U_m$ | Mean potential velocity |
| $\rho$ | Density |
| $\nu$ | Kinematic viscosity |
| $p$ | pressure |
| $\tau_w$ | Wall shear |
| $\delta^*$ | Displacement thickness. |
| $\delta^{**}$ | Energy thickness |
| $\theta$ | Momentum thickness. |
| $H$, $L$ | Shape factors associated with turbulent boundary layer solutions. |
| $m$ | Shape factor associated with laminar boundary layer solutions. |
| $x$ | Denotes position on blade. |
| $c$ | Chord |
| $y_{tA}$ | Half the profile thickness at the point of separation. |
| $\theta$ | Camber angle. |
| $S$ | Space between two consecutive blades in the cascade. |
| $\beta$ | Blade angle. |
| $\alpha$ | Flow angle. |
| $\alpha_m$ | Mean flow angle. |
| $i$ | Incidence |
| $C_p$ | Coefficient of pressure. $\left(= \frac{p-p_1}{\quad}\right)$ |

| | |
|---|---|
| $\sim$ | Shape factor for laminar region ($= \frac{\theta^2}{\nu}\frac{du}{dx}$) |
| $C_f$ | Local skin coefficient of friction. |
| $C_D$ | Coefficient of drag. |
| R | Body Reynolds number ($= \frac{U_\infty c}{\nu}$) |
| $Re_x$ | Reynolds number based on chordwise position. ($\frac{U x}{\nu}$) |
| $Re_\theta$ | Reynolds number based on momentum thickness. ($\frac{U\theta}{\nu}$) |

**Suffices**

| | |
|---|---|
| A | Indicates point of seperation. |
| TS | At trailing edge on suction side. |
| TP | At trailing edge on pressure side. |
| TE | At trailing edge. |
| $t_r$ | For transition. |
| i | For instability. |
| m | For mean. |
| 1 | For inlet. |
| 2 | For exit. |
| Corr. | For corrected. |

## 1. INTRODUCTION

A detailed theoritical and experimental study of flow through cascade isrequired for a real progress in the solution of fluid mechanics problems of turbomachines. These studies play a prominent role in turbomachines of all types.

In two dimensional cascade flow, boundary layers develop on both the suction and pressure surfac -es of the blade. These surface boundary layers then come together at the blade trailing edge and form the blade wake. As the wake moves down stream, a mixing takes place between the wake and free stream, and through viscous action, the flow becomes uniform at some distance behind the blade trailing edge.

Although in many practical problems, the blade surface boundary layer constitutes a small portion of the flow field, it plays a decisive part in the determination of the actual flow characterstics of the cas-cade . The effect of blade boundary development on cascade losses is obvious. Since the resulting wake formation contains a defect in total pressure. The surface boundary layer can also exert a strong influence on thesurface pressure distribution and outlet angle characterstics of the blade. If the boundary layer is very thin, the pressure distribution obtained from potential flow calculations over the

original body will be a good approximation to the actual distribution. As the boundary layer thickens, however, the actual pressure distribution will depart from the potential flow determination. Under certain conditions, the boundary layer actually separates from the surface of the blade somewhere before the trailing edge. Under such circumstances the entire flow pattern about the cascade is altered by the displacement of fluid accompanying such separation, and the potential flow solution about the original profile looses its significance almost completely. Therefore it is obvious that only a theory of viscous flow through cascade can answer such important questions as to how the smallest possible loss coefficient and the best possible efficiency can be obtained, and by what mechanism stall effects the efficiency of a turbomachine

This report is an extension of a work done by Murali Mohan, who dealt with the theoritical prediction of scale effect on an axial fllw fan. Scale effect is encountered when the performances of two machines, with different sizes and having the same shape are compared. It is known that the geometrically similar machines are said to have Reynolds similarity when they have the same Reynolds Number. Thus the study of variation of properties with Reynolds number is equivalent to the study of the size effect on those properties.

The theoritical investigation of Reynolds number effects on the performance of an axial flow fan blading can be done by means of computations of the boundary layer growth for typical fan blade velocity distribution. Thereafter the momentum defect thickness at the trailing edge may be obtained to give values of the overall blade drag. The estimation of the point of transition from laminar flow to turbulent flow affects the boundary layer parameters at the trailing edge. This report uses Michal's criterion for locating the transition point on the blade surfaces. The results of overall blade drag are compared with those of Murali Mohan and also with the well known formulae given by Squire & Young for isolated aerofoils.

## 2. LITERATURE SURVEY

The analysis of viscous flow through cascade enables us to find out the aerodynamic loading of compressor blade sections. It is obvious that the seperation of the boundary layer will result in an increase in the losses, causing a reduction in efficiency.

The boundary layer on a blade may consist of several regions starting with a laminar boundary layer The laminar layer may seperate from the surface either fully of partly. In the later case it re-attaches after a region of separated flow. It may be mentioned that the turbulent boundary layer may also seperate from the surface. Seyb (5) has listed the following factors which influence the state of the boundary layer

Pressure gradients.

Turbulence.

Reynolds Number.

Shock/boundary Layer interaction

Mach number

Surface roughness

Surface curvature

Temperature gradients

Suction or blowing

Condition at "start" of boundary layer

Passing wakes or unsteady flow

Three dimensional effects.

The first step is to calculate the velocity distribution round the blade for the range of inflow angles of interest. The well known Martenson method may be used for this

The next step is the calculation of the boundary layer parameters corresponding to these velocity distributions for the following parts :

a) Laminar boundary layer
b) Turbulent boundary layer
c) Laminar separation point or transition point / re-gion and bubble size
d) Turbulent boundary layer separation point
e) Local heat transfer coefficients

Many earlier studies e.g. Schlichting ( 18 ), Schlichting & Scholz (19) etc. are based on the assumption that turbulent flow starts from the leading edge. In some experimental cases transition point is created by introducing a trip wire at the leading edge. However in actual practice there will be some region of laminar boundary layer on the blade surface.

The existance of this region has been confirmed recently by Walker (1), Horlock (21), has also mentioned the above refrence and explains the importance of further study of the above mentioned aspect. Walker (1) has studied the boundary layer development on theb blades of the stator of a single stage axial

on the blade of the stator of a single stage axial flow compressor. There is a marked region of laminar boundary layer even for the high turbulence intensity caused due to the presence of the rotor. Bobb (43) has also studied the boundary layer development on the blades of a compressor cascade. He used 10C4 | 30C50 and 10C4 | 50C50 blades with stagger of 20° and aspect ratio of 2. The incidence was varied from -5° to 10° oil film technique for flow visualization was also adopted by him. He also confirmed that there was a laminar region on blade surfaces for various incidences Quadir (16) has also measured boundary layer parameters on a low aspect ratio compressor cascade of high camber. His results confirm the view of walker (1).

The complete viscous flow about cascade sections is generally considered to be described by the equations Navair -Stokes and the continuity equations. For two dimensional incompressible flow neglecting body forces, these equations are written as follows :

$$\left.\begin{aligned} \frac{\partial u}{\partial t} + \frac{u\partial u}{\partial x} + \frac{v\partial u}{\partial y} &= \frac{-1}{\rho}\frac{\partial p}{\partial x} + \nu\left(\frac{\partial^2 u}{\partial x^2} + \frac{\partial^2 u}{\partial y^2}\right) \\ \frac{\partial v}{\partial t} + \frac{u\partial v}{\partial x} + \frac{v\partial v}{\partial y} &= \frac{-1}{\rho}\frac{\partial p}{\partial y} + \nu\left(\frac{\partial^2 v}{\partial x^2} + \frac{\partial^2 v}{\partial y^2}\right) \\ \frac{\partial u}{\partial x} \quad \frac{\partial v}{\partial y} &= 0 \end{aligned}\right\} \quad (2.1)$$

The last equation represents the condition of continuity. The Euler equations for non-viscous fluids can be obtained by setting the kinematic viscousity equal

The solution of equation (2.1) has not been found in any but the simple cases of Laminar flow. A solution for the flow through an arbitrary cascade is not feasible at the present time. However, when the predominant viscous efforts are confined to the boundary regions, a simplifying approximation is possible. By considering relative magnitudes (within the boundary Layer ) of the terms appearing in equations ( 2.1 ) that system of equations can be reduced to the following :

$$\left.\begin{aligned} &\frac{\partial u}{\partial t} + \frac{u\partial u}{\partial x} + \frac{v\partial u}{\partial y} = \frac{-1}{\rho}\frac{\partial p}{\partial x} + \nu\frac{\partial^2 u}{\partial x^2} \\ &\frac{\partial u}{\partial x} + \frac{\partial v}{\partial y} = 0 \end{aligned}\right\} \quad \text{---- (2.2)}$$

The boundary layer is assumed sufficiently thin and the curvature of the surface sufficiently small that the pressure gradient normal to the surface is negligible within the boundary layer can be determined from the potential flow outside the boundary layer. Equations (2.2) represent a significance simplification of equations (2.1) and have proved reliable in many flow problems. Unfortunately , these equations, also, are very difficult to solve in most cases ofpractical interest.

A decisive simplification in approach was made by Von Kármán, who integrated the first of the equations

( 2.2 ) with respect to Y and thus replaced the boundary layer equation with an integral condition that can be written in the following form :

$$\frac{\tau_w}{\rho U^2} = \frac{d\theta}{dx} + \frac{\theta}{U}(2+H)\frac{dU}{dx} \quad \ldots\ldots(2.3)$$

where U is the velocity at the outer edge of the boundary layer and $\tau_w$ is the surface shear stress. In this manner, the boundary layer equations are required to be satisfied only in the mean instead of at each point along normal to the surface in the boundary layer region. Equation ( 2.3 ) has provided the basic equation for most of the general boundary layer investigations.

Many theories have been developed from equation (2.3) for approximately solving the boundary layer problem with pressure gradient for both laminar and turbulent flows. These theories although not completely successful, provide some orderly means of attacking the problem for either the laminar or the turbulent layer.

## 2.1 Laminar Boundary Layer

There are many methods of calculating the laminar boundary layer parameters such as Thwaites ( 11 ) Walz ( 11 ), Loĭtsianskiĭ's ( 11 ) etc. All the methods have similar expressions for finding out the growth of momentum thickness except the numerical constants. It is interesting to note that the predicted

boundary layer momentum thickness is very close to the experimental values as concluded by many investigators like Walker (1), Bobb (43), Quadir (16) etc. Bobb (43) has used Wals method, whereas Walker (1) and Quadir (16) have used Twaite's method. The description of Twaite's method istherefore necessary for the completeness of the problem, which is given below :

Assuming that the velocity profile in the two dimensional laminar boundary layer may be represented by a single parameter m, the boundary layer momentum integral equation (2.3) reduces to the form

$$\frac{U}{\nu}\frac{d(\theta^2)}{dx} = F(m) \qquad (2.4)$$

Where m is defined as

$$m = \frac{-\theta^2}{\nu}\frac{dU}{dx} \qquad (2.5)$$

Twaite's examined all known exact solutions and accurate computations of the laminar boundary layer and found that in no case did the function F (m) depent far from the straight line

$$F(m) = 0.45 + 6\,m \qquad (2.6)$$

Replacing F (m) by this linear relation; equation (2.4) leads to an explicit relation for the boundary layer

momentum thickness in terms of the surface velocity distribution :

$$\frac{\theta^2}{\nu} = \frac{0.45}{U^6} \int_0^x U^5 \, dx \qquad (2.7)$$

For finding out the other parameters of the laminar boundary layer one may use the table provided by Twaites for the purpose. The above equation may be written in non dimensional form as

$$\left(\frac{\theta}{c}\right)^2 \left(\frac{U_m c}{\nu}\right) = \frac{0.45}{(U/U_m)^6} \int_0^{x/c} \left(\frac{U}{U_m}\right)^5 d\left(\frac{x}{c}\right) \qquad (2.8)$$

## 2.2 Laminar seperation point or transition region / point and bubble size

It is particularly important to determine the "point" and process by which the boundary layer changes from a laminar to a turbulent state as this can have a significant effect on the aerodynamic performance of the cascade and a local heat transfer rates.

The research on transition process is in such a state that we can still present only a rather feable progress report. White ( 27 ) has remarked that the final report on transition, indeed, may never be handed in. Historically evidence has not been gathered in cumulative fashion, the bulk of opinion about transition swaying drastically from one misconception to another. The Raleigh inviscid theories threw up a smoke screen about the real culprit : resistive infinitesimal instability. Then, when the two dimensional Tollmien - Schlichting waves were finally pfedicted, researchers ignored them because the overwhelming bulk of experiments pointed clearly to transition as a three dimensional "explosion" into turbulence. Years later, when Schubauer and Skramstad (6) and also Liepmann (28) documented the Tollmien-Schlichting waves, the rush of opinion to embrace the two dimensional cause was so great that Liepmann's clear indication of spanwise fluctuations was entirely ignored. A decade later, Emmons (25) accidentally noticed sporadic turbulent spots on shallow running water; two dimensionality was abandoned and suddenly, as Morkovin ( 26 ) wryly notes, "everyone was seeing spots". It was another decade before Klebanoff, Tidstrom, and Sargent (24) clarified the essential intermediate process involving longitudinal vorticity & spanwise energy exchange. Added to this is the annoying unit Reynolds number effe -ct , by which transition process differ among the vario

for the initial disturbance spectrum ( free stream turbulence, radiated noise, surface roughness ) on the actual paths toward turbulence. The complexities of these parameters and their interactions continue to discharge our hopes for a definitive picture of the transition process.

Most methods of predicting transition point have concentrated on the low speed, smooth wall, and quiet flow with variable pressure gradients such as an aerofoil in free flight. The first such method, due to Schlicting and Ulrich ( 29) is simple and still very popular. In this method two positions are important ;

1) The point of instability $x_i$, where unstable Tollmien Schlicting waves first appear and
2) The ultimate transition point $x_{tr}$ , when the flow becomes the fully turbulent.

One computes $x_i$ from the laminar instability theory and then computes the remaining distance $(x_{tr} - x_i)$ from a correlation due to Granveill (9). White (27) has given an empirical formulae for the above correlation as

$$Re_\theta(x_{tr}) \approx Re_\theta(x_i) + 450 + 400 e^{60\lambda_m} \qquad (2.9)$$

where

$$\lambda_m = \frac{1}{x_{tr} - x_i} \int_{x_i}^{x_{tr}} \lambda(x)\, dx \qquad (2.10)$$

It may be noted that for a favourable pressure gradient ( $\lambda_m$ ) the last term of equation ( 2.9 ) is very large and therefore the transition point

is far down stream. This isexpected due to the high stability of the favourable profiles. Conversely in a separating flow ( $\lambda_m \approx -0.1$ ) the last term of equation ( 2.9 ) is negligible which shows that $x_{tr}$ is very close to $x_1$ .

Dunham ( 30 ) has attempted to formulate a basis for prediction of boundary layer transition on turbomachinary blades. He used the data of Evans (31) Turner (32), Apostolopoulo (33), Wilson & Pope (34), Dunham & Edwards (35), Pollard & Gostelow (36) and Walker (37). He has mentioned that two distinct forms of transitions have been commonly observed :

a) "Natural Transition": a gradual increase in the proportion of the flow, which is turbulent at any instant ( Intermittancy ) from 0 to 1 ; and

b) "Bubble transition" : A laminar separation bubble followed by reattachment as a turbulent boundary layer

Dunham (30) in his paper has mentioned about the work of Hall & Gibbings (44) also, who has reviewed the various methods of predicting transition. Dunham has also summarized the work of Horton (48) which gives a semi empirical theory for the growth and bursting of laminar separation bubbles. He goes on to say:

> " the general conclusion is unavoidable that the present prediction methods remain uncertain and that many careful experiments are

needed if reliable methods are to be established.

White ( 27 ) has recommended the use of Michel's method of predicting transition untill a demonstrably more rigorous procedure arrives. He has given an empirical expression for Michel's data ( using curve-fitting technique ) as

$$R_{e\theta} \approx 2.9\, R_{ex}^{0.4} \qquad (2.1)$$

Murali Mohan ( 30 ) has predicted the points of transition on the basis of the instability of the laminar boundary layer. For this the local Reynolds number based on the displacement thickness i.e. $\frac{U\delta^*}{\nu}$ is evaluated along the chord of the blade, which is increasing in nature as the displacement thickness increases towards trailing edge. But as the universal trend in the relation between $(\frac{U\delta^*}{\nu})_{critical}$ and the shape factor $\lambda$ exists, which is got from the stability consideration of the boundary layer equations. So for every point along the blade chord the value of $(\frac{U\delta^*}{\nu})_{critical}$ is calculated corresponding to the local value of shape factor. The flow is said to be stable if the local value of $\frac{U\delta^*}{\nu}$ is less than the critical value obtained by above method. Proceeding along the laminar boundary layer in the down stream direction from the foreward stagnation point at an assumed constant body Reynolds

in pressure. But on the other the boundary layer is thin and consequently the local Reynolds number $\frac{U\delta^*}{\nu}$ is small. Therefore the boundary layer is stable. As going on further downstream, the pressure is found to be decreasing at lower lower rate, till there is pressure increase behind the point of minimum pressure. Hence the local limit of stability $\left(\frac{U\delta^*}{\nu}\right)_{critical}$ decreases continuously downstream, where as the local Reynolds number $\frac{U\delta^*}{\nu}$ increases continuously. Finally a point is reached where

$$\frac{U\delta^*}{\nu} = \left(\frac{U\delta^*}{\nu}\right)_{critical} \qquad \text{---------- ( 2.12 )}$$

This point is known as point of instability. From this point onwards the boundary layer is unstable. Its position is evidently a function of the Reynolds number $\frac{U_m c}{\nu}$ since it ( Reynolds number ) influences the local boundary layer thickness. Murali Mohan (20) has taken this very point of instability as the point of transition. While the point of transition lies downstream of the point of instability. He has also mentioned that the distance of separation between the theoritical point of instability and the experimental point of transition varies from case to case.

Walker ( 1 ) also treated the phenomenon of transition not as an instantstaneous one but as a region. He developed a new scheme of predicting transition which better described the observed behaviour at low Reynolds numbers and higher adverse pressure gradients

found in the compressor. He divided the transition process in two regions:

1) An "instability region", defined as extending from the point of neutral stability of the laminar boundary layer to small two-dimensional disturbances, to the point at which localised regions of turbulent flow first appear; and
2) A "transition region", in which the intermittency of turbulence increases from zero to one due to the spreading of localised spots of turbulent flow.

The point of neutral stability to small two-dimensional disturbances in the laminar boundary layer was determined from the curve of critical boundary layer Reynolds number $R_{e\theta\ crit.}$ against pressure gradient parameter K, given by Rosenhead (11) as the mean of calculations by a number of workers. The end of the instability region, which will be called transition point, was inferred from the decrease in boundary layer shape factor H, the increase in skin friction and noise level which result from the onset of the turbulent mixing. The error in locating this point is thought to have been less than 2% of chord in most cases. The end of the transition region, where the boundary layer flow became continuously turbulent, was indicated by the stabilisation of shape factor, skin friction and noise level to values characteristic of turbulent

instability and transition reions are about 40% and 20% of the chord respectively.

## 2.3. Turbulent Boundary Layer

Once the transition point is estimated the next step is to calculate the turbulent boundary layer growth. There are many methods of computing the incompressible two-dimensional turbulent boundary layer. In general such analysis can be divided into two types;

1) Integral methods arranged across the boundary layer, and
2) Finite difference, or differential methods which attempt to solve the full partial differential equations of the boundary layer.

In 1968 a conference was held at Stanford which provided a splendid source of well-purified boundary layer data {(Coles & Hirst (38)} for a direct check on the accuracy of the various methods. One of the conclusion of the conference was that in no way the integral methods were inferior to the differential methods for the cases they considered. Considering the time of computation involved and the foregoing conclusion many earlier researchers have used integral methods for the purpose.

Smith (39) has used five methods of predicting

the incompressible, two-dimensional turbulent boundary layer to flow conditions considered to occur over the suction surface of turbomachine blades. He has also assessed the agreement between the separation criteria and boundary layer characteristics. The methods considered were those due to Buri (18)*, Truckenbrodt (18)*, Stratford (40), Maskell (41) and Spence (42)*. He concluded that:

1) All of the criteria could be brought into tolerable agreement provided that value of 'm' -0.04 was used for Buri's criteria, and that for Truckenbrodt and Spence's methods the position of separation was determined by the condition thatlocal skin friction coefficient is zero. It was additionally necessary in the methods of Maskell, Truckenbrodt and Spence for the calculation of the shape parameters to be started with a value of 'H' as 1.4.

2) All of the criteria except Spence's were sensitive to Reynolds number and showed that an increase in Reynolds number delays separation.

3) Stratford's method was extremely easy to apply, was the simplest of the five and predicted the lowest pressure rise to separation.

---

* Book reference is given.

4) To assist in the design of blade profiles envelops of suction surface velocity distribution have been constructed to give separation at the trailing edge; these are considered to be conservatively based.

Pollard & Costelow (36) also measured the boundary layer development on a 6 inch chord blade under the conditions of leading edge roughness, and obtained fair success in predicting the boundary layer growth using the simple calculation methods derived by Truckenbrodt.

Horlock (22) has discussed that the methods of calculating turbulent boundary layer will give adequate prediction of the layer over a substantial area of the blade surfaces, if turbulent flow develops quickly near the leading edges, as is the case in most high speed axial flow compressors. He has further mentioned that the prospects of accurate calculations of turbulent separation under the complex conditions existing in compressors seem somewhat remote.

The results of Bobb (43) and Quadir (16) also show that for moderate loading Truckenbrodt's method predicts momentum thickness growth satisfactorily except near the trailing edge.

The method due to Truckenbrodt is explained below.

## TRUCKENBRODT METHOD

In calculating the momentum thickness Truckenbrodt followed a different path that followed by others i.e. he made use of the energy integral equation for obtaining the expression of turbulent boundary layer (momentum thickness). The energy integral equation is :

$$\frac{d}{dx}\left(U^3 \delta^{**}\right) = 2\nu \int_0^\infty \left(\frac{\partial u}{\partial y}\right)^2 dy \qquad (2.13)$$

where $\delta^{**}$ denotes the energy thickness, defined as

$$\delta^{**} = \int_0^\infty \frac{u}{U}\left[1-\left(\frac{u}{U}\right)^2\right] dy \qquad (2.14)$$

Truckenbrodt found, after evaluating with different experimental data, that the following expression holds good for the turbulent boundary layer.

$$\theta \left(\frac{U\theta}{\nu}\right)^{\frac{1}{n}} = \frac{C_1 + A\int_{x_{tr}}^{x} U^{3+2/n}\, dx}{U^{3+2/n}} \qquad (2.15)$$

where the value of ' $n$ ' can be taken as 4 for small Reynolds number and 6 for large Reynolds number '$C_1$' is a constant which takes into account the laminar portion of the boundary layer; 'A' is also a constant which can be taken as 0.0076 and $x_{tr}$ is the point of transition..

In cases when the boundary layer does not separate the calculation of the momentum thickness $\theta$ (x) along the contour of the body essentially completes the calculations of the turbulent boundary layer. But since the turbulent boundary layer seperation is always expected at large Reynolds number and at greater incidences, so to find the position of the seperation along the contour, Tuckenbrodt introduced another new shape factor L defined as :

$$L = \int_{\bar{H}=\bar{H}_0}^{\bar{H}} \frac{d\bar{H}}{(\bar{H}-1)\bar{H}} \qquad (2.16)$$

where $H = \delta^*/\theta$ and $\bar{H}=\delta^{**}/\theta$. The lower limit of integration in equation ( 2.16 ) has been so choosen as to make $L = 0$, corresponds to the case of zero pressure gradient (flat Plates) i.e. $\bar{H}=\bar{H}_0 \approx 1{\cdot}73$ and $H_0 = 1{\cdot}4$.

finally he got the result for L as below:

$$L = \frac{\xi_{tr}}{\xi} L_{tr} + \ln\frac{U(\xi)}{U_{tr}} + \int_{\xi_{tr}}^{\xi} \left[ b(\xi) - \ln\frac{U(\xi)}{U_{tr}} \right] d\xi \qquad (2.17)$$

He expressed 'b' in terms of momentum thickness with the following approximation

$$b_{\xi} = 0.07 \log_{10} \left( \frac{U\theta}{\nu} \right) - 0.23 \qquad (2.18)$$

and $\xi$ is defined as

$$\xi = \left[ C_1^* + \frac{A}{R^{1/n}} \int_{x_{tr}/c}^{x/c} (U/U_m)^{3+2/n} d(x/c) \right]^m \qquad (2.19)$$

where $C_1^* = \dfrac{C_1 \nu^{1/n}}{(c\,U_m)^{1+1/n}}$

$R$ is the body Reynolds number ($=\frac{U_\infty c}{\nu}$), the suffix 'tr' indicates the transition point, and the values of m and n are 4 and 6 respectively. Separation occurs for $L_m$ = - 0.13 to -0.18, which correspond to H = 1.8 to 2.4.

He also assumed that shape factor (H) has little effect on the growth of the momentum thickness and was taken as being constant and equal to 1.4.

## 2.4. Drag Coefficient

Speidel & Scholz (17) have given an expression for finding out the loss coefficient, deflection coefficient, the drag coefficient etc. for a two-dimensional cascade. As discussed earlier, the loss coefficient can be obtained from viscous flow theory only. The drag coefficient is related to it in terms of loss coefficient as { Vasandani (23) }

$$C_D = \frac{s}{c} \zeta_v \sin^3 \beta_\infty \qquad (2.20)$$

where the loss coefficient $\zeta_v$ is obtained from:

$$\zeta_v = \frac{2\Theta}{\sin^2 \beta_{2\,corr}} \qquad (2.21)$$

Here $\Theta$ denotes the dimensionless momentum thickness which is obtained from the momentum thicknesses at the trailing edge of the blde. $\beta_{2\,corr}$ is the angle of flow at outlet in the [illegible] potential flow, which has been

It is worth mentioning that the losses associated with a cascade consist of losses in the unseparated boundary layer, of additional losses due to separation (if any), and of losses due to turbulent mixing in the wake.

When there is no separation on the blades, the dimensionless momentum thickness is given by

$$\bar{\theta} = \frac{\theta_{TS} + \theta_{TP} + \theta_A}{s \sin \beta_2 \, corr} \qquad (2.22)$$

where $\theta_A$ is an additional momentum thickness due to additional loss caused by separation ( hence for unseparated flow $\theta_A = 0$ ) and is given by Speidel & Scholz (17) as

$$\theta_A = \frac{1}{2} y_{tA} \left\{ (U_A/U_2)^2 - 0.9 \right\} \qquad (2.23)$$

$y_{tA}$ means half the profile thickness at the point of separation and $U_A$ the potential fllw velocity at the point of separation A. The criterion for the point of separation has already been discussed earlier.

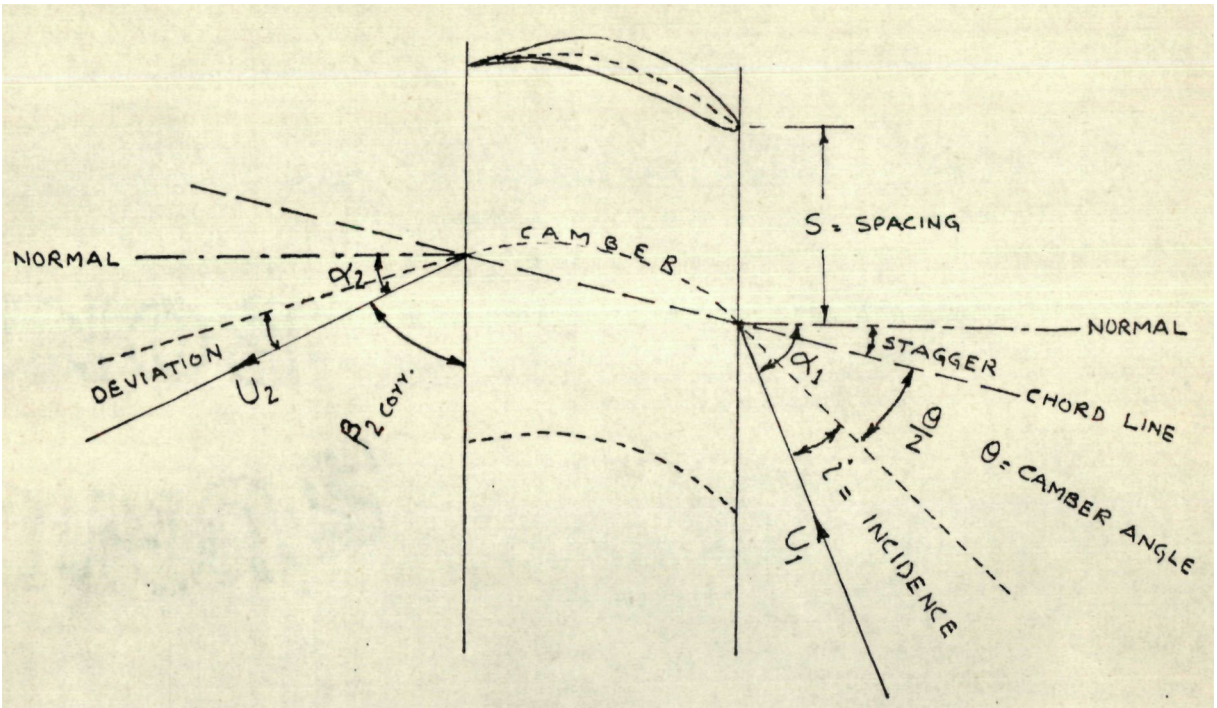


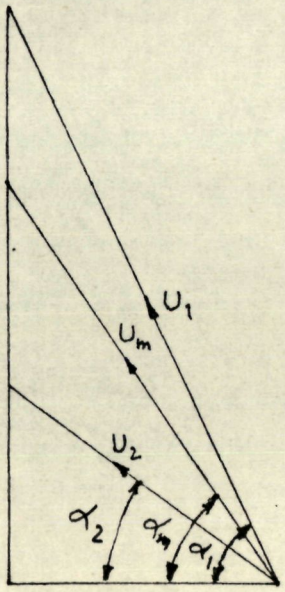


CASCADE FLOW DIAGRAM

## 3. PROGRAM OF STUDY

As discussed in the earlier chapter, the first step in the boundary layer computation is the calculation of the velocity distribution around the blade for the range of inflow angles of interest. The present study takes the velocity distribution as found out experimentally for a cascade test conducted at the University of Edinburgh as reported by Murali Mohan (20). For this, experimental plots of non-dimensional pressure coefficient $C_{pl}$ against the non-dimensional chordwise position along the blade, x/c for the incidences to be considered are used. The pressure plots are converted into non-dimensional velocity plots using the Bernoulli's equation. The details of cascade are as follows:

Blade Profile : 10 C 4
( Circular arc camber )

Camber angle, $\theta = 30^\circ$

Stagger = $37^\circ$

Blade inlet angle, $\beta_1 = 52^\circ$

Blade exit angle, $\beta_2 = 22^\circ$

Space chord ratio, S/c = 0.75

Aspect ratio , h/c = 2.0

The incidences that are considered are

(i) $i = 10^\circ$

(ii) $i = -2^\circ$

For incidence $i = 10^{\circ}$

$\alpha_1$ = flow angle at entry to the cascade = $62^{\circ}$

$\alpha_2$ = flow angle at exit to the cascade = $29.75^{\circ}$

For incidence $i = -2^{\circ}$

$\alpha_1$ = flow angle at entry to the cascade = $50^{\circ}$

$\alpha_2$ = flow angle at exit to the cascade = $26.5^{\circ}$

Let the flow angle corresponding to the cascade mean flow be $\alpha_m$.

Since $\tan \alpha_m = \frac{1}{2}( \tan \alpha_1 + \tan \alpha_2 )$

therefore for $i = 10$, $\alpha_m = 50^{\circ} 48'$

for $i = -2$, $\alpha_m = 40^{\circ} 12'$

The main problem in the present study is the estimation of the momentum thickness on blade surfaces at the trailing edge ( as momentum thickness is a measure of the losses in the flow ). The entire computation work is carried out on IBM 1130 computer installed at A.M.U. computer centre. Computer programs were developed for

(a) inter-polation of $C_{p1}$ values at intermediate points of calculation using cubic spline method. This program also gives the values of first derivatives at the points considered.

(b) the Thwaites method for laminar boundary layer calculation.

(c) transition point estimation using Michel's criterion.

The results obtained are compared with those of Murali Mohan (20) and also with the results obtained by Squire & Young method.

## 4. RESULTS AND DISCUSSIONS

First ofall the non-dimensional pressure plots are converted into non-dimensional velocity plots. If U is the potential velocity at any chord position x/c where the coefficient of pressure is $C_{p1}$ and $U_1$ the free stream velocity for upstream of a cascade, then the following relation is valid.

$$\left(\frac{U}{U_1}\right)^2 = 1 - C_{p1} \qquad (4.1)$$

$$\text{Now} \quad \left(\frac{U}{U_m}\right) = \frac{U}{U_1} \cdot \frac{U}{U_m} \qquad (4.2)$$

Where $U_m$ is the vector mean velocity through the cascade. Further from continuity equation

$$U_1 \cos\alpha_1 = U_m \cos\alpha_m \qquad (4.3)$$

Therefore

$$\frac{U}{U_m} = \left(1 - C_{p1}\right)^{\frac{1}{2}} \frac{\cos\alpha_m}{\cos\alpha_1} \qquad (4.4)$$

Figure 1 gives two -dimensional static pressu -re distribution for incidences of $10^o$ and $-2^o$ in terms of $C_{p1}$ against x/c . Equation (4.4) along with the data obtained from figure -1 gives usthe non-dimensional velocity plots as shown in figure . It is found that in general for all the four cases the velocity plots are smooth in nature. Further the flow is accelerated

because of the greater rate of change of velocity.

The values of the coefficient of pressure for different values x/c are interpolated by putting a cubic spline for the data available from the experimental plots. at equal interval. As already mentioned a computer programe was developed for the above method. The cubic spline method also gives the first derivative at any point of consideration. It may be mentioned that for solving the simultaneous algebraic equation as required in the cubic splinemethod, The end condition are to be specified. Pennington (4) has specified that third derivative are continuous at the end point of the curve. The present study tried these boundary conditions but the results obtained were not satisfactory. The end conditions were then modified in order to get smooth results of the first derivatives at thepoint of interest. The second derivatives at the end points are considered to be zero in the modified programe. These end conditions necessarily mean that the spline is hinged freely at the end points. The graph obtained by this method for the coefficient of pressure is given in figure

After finding out the velocity distribution the boundary layer calculation was started in steps as mentioned in chapter 3. The experimental results are under natural transition and therefore the turbulent boundary layer calculation right from the leading edge is not carried out. Walker (1) has

exist on turbomachine blading inspite of the high level of disturbance from the wakes of upstream blade rows. The earlier assumption that the boundary layer in turbomachinary would be almost universally turbulent, probably originates largely from observations of transition on flat plates. It is to be noted that for flat plates, for free stream turbulence levels of about 2%, the onset of turbulent flow becomes almost coincident with the calculated point of laminar instability. For this reason, many theoritical analyses of cascade performance have assumed the turbulent flow to originate at the blade loading edge.

Thwaites method of laminar boundary layer calculations was programmed for IBM 1130 computer and the computed results are shown in figures (3A) (3B) (3C) (3D). As is obvious the momentum loss should increase along the chord which is being clearly shown in the above figures. The momentum loss on the suction side should be naturally more than on the pressure side, because of the greater adverse pressure gradient on the former. Further more the losses should increase when the incidence is increased. These are indicated by the $(\frac{\theta}{C}) R^{1/2}$ vs. $x/c$ plots.

While discussing the results for finding out the transition point on the blade surfaces, it is worth mentioning the results on an isolated aerofoil as explained by Schlichting (18). He has deduced the rule on a rough basis that the point of transition almost coincides with the point of minimum pressure of the potential flow in the range of Reynolds numbers from $10^6$ to $10^7$. At very large Reynolds numbers the point of transition may lie a short distance infront of that position and it may move a considerable distance behind it at small Reynolds numbers particularly when the pressure gradient whether +ve or -ve, is small. Further it is observed that the point of transition always lies infront of the point of laminar seperation, irrespective of the values of the Reynolds numbers. Thus the rule may be established that the point of transition lies behind the point of minimum pressure but infront of a point of laminar seperation, at all except very large Reynolds numbers.

However the situation in the case for flow through cascades appears to be different than the above mentioned results. In the present study the following typical results are presented for a Reynolds number of $10^5$.

Incidence = $10^0$ , suction side

Point of minimum pressure = 0.035

The effect of Reynolds numbers on pressure distribution may be prominent for the lower values. The present study as well as that of Murali Mohan ( 20 ) does not take this variation because of the absence of experimental pressure plots. The position of the laminar separation point will therefore not vary with the variation of Reynolds numbers. This may be explained as

$$m = \frac{-\theta^2}{\nu} \frac{dU}{dx}$$

or

$$m = -\left(\frac{\theta}{c}\right)^2 \frac{U_m c}{\nu} \frac{d(U/U_m)}{d(x/c)} \qquad (4.5)$$

In the above expression the term $\left(\frac{\theta}{\nu}\right)^2 \frac{U_m c}{\nu}$ is purely a function of velocity distribution as given in ( 2.8 ). Hence the pressure gradient parameter m is also a function of velocity distribution only. The corresponding value of the chord for m =-0.082 is therefore independent of Reynolds number ( $\frac{U_m c}{\nu}$ ).

The point of transition as given by Nicholl's criterion moves towards the leading edge when Reynolds number is increased, as is expected. For the case, illustrated above, it is interesting to note that the point of transition almost coincides with point of laminar seperation at Reynolds number $10^7$. For values of Reynolds numbers greater than $10^7$ the transition points were in front of a laminar seperation point. The variation of transition point

These
in figure ( 5A ) that is an absence of predicted points of transition for the pressure side for Reynolds number $\leq 10^6$. Under such a Reynolds number range the boundary layer on pressure surface for $10^0$ incidence remains laminar right upto the trailing edge. This conclusion is based on the results given by the Michel's criterion. The method of Michel is to plot $Re_\theta$ against $R_{ex}$ along the surface until the curve passes a critical point at which transition is assumed to occur, the position of the critical point being found from a plot of $Re_{\theta\ tr}$ against $Re_{x\ tr}$ of previous experimental results. The present study avoids the above plot and instead uses equation (2.11). Hall & Gibbing ( 44 ) while discussing the method of Michel has pointed out the criticsms of Crabtree (45) and Smith & Gamberoni (46) about the low accuracy of Michel's method. It is of interest to note that the version of Michel's curve reproduced by Crabtree (45) is very close to a plot of $Re_\theta$ against $Re_x$ for the zero pressure gradient boundary layer given by the Blassius solution , $Re_\theta = 0.664\ Re_x^{0.5}$ . Thus the point of transition has to be found from the intersection of two nearly parallel lines, which means that small errors in the calculation results in large error in the transition point prediction. The reason for the absence of the points of transition on pressure surface

for $10^{o}$ incidence for Reynolds numbers $\leq 10^{6}$ may be given in the light of the above discussion.

After locating the point of transition the turbulent boundary layer was started using the well known simple quadrature method of E. Truckenbrodt. For finding out the integrals associated in the above method, first of all, trapezoidal rule of numerical integration was used. The momentum thickness distribution as predicted by the above method is plotted in figures ( 6A ) ( 6B ) ( 6C ) ( 6D ). The prediction of theshape factor ( $H = \delta^{*}/\theta$ ) involves careful integration which was observed as at a later stage during calculation. As discussed earlier there is a correlation between H and L (another shape factor) which is given in the form of a graph. In order to check the correctness of the computer programme developed, calculations were performed for the known results given by Smith (39). While comparing the results, the momentum thickness variation was perfectly alright. However, there was discrepancy in the computed values of H withthe results given by Smith(39). After investigation it was found out that the Trapezoidal numerical technique did not work satisfactorily in the above scheme. The integral equations were then converted into ordinary differential equations and a standard routine of Runge-Kutta-Gill method was employed for their solutions. With the introduction of the above

agreement with the results given by Smith (39). Having established the accuracy and correctness of the developed programme, calculations were performed for the studies under consideration.

It may be mentioned that the initial value of factor H , was specified as 1.4. The corresponding value of $\lambda$ is zero. This is based on the recent observation carried out by Quadir (16) at I.I.Sc Bangalore. He has concluded that the value of shape factor for different incidence angles at the point of transition is almost equal to 1.4. This value of shape factor is also taken for turbulent boundary layer calculation on flat plates. The computed results are plotted in figure ( 7 ) for different Reynolds number.

Generally the turbulent boundary layer is considered to seperate from the surfaces at values of H between 1.8 to 2.4. Truckenbrodt has given the limiting values of $\lambda$ between -0.13 to -0.18. These values are based on many earlier experiments carried out under two-dimensional conditions. The results for cascade flows are lacking in literature. However Quadir (16) while measuring the boundary layer development on blade surfaces has come across the turbulent boundary layer separation towards the trailing edge at moderate blade loading. He has further concluded that the value of H as high as 4.3 was observed at the point of separation. This was confirmed from the nature of

velocity profiles as well as with the help of chicken down used for flow visualization technique. In the present study the value of $\lambda$ at separation was therefore, taken to be -0.20 in order to accomodate higher value of the shape factor H. Based on this criterion it was observed that the boundary layer was fully attached for lower Reynolds numbers. As the Reynolds number increases the existance of boundary layer separation is predicted. For further increase of Reynolds number the turbulent boundary layer separation disappears from the scene.. In order to understand a clear picture for the prediction of turbulent boundary layer separation the variation of the shape factor $\lambda$ against chord wise position for different Reynolds numbers was plotted for 10° incidence on suction surface as shown in figure ( 7 ) It is apparent that $\lambda$ decreases towards the trailing edge. Further in the above figure the curve for lower Reynolds number is more steep than that for higher Reynolds number. It may be noted from the curve drawn that the $\lambda$ variation approached or intersected the line marked for separation for only three Reynolds numbers whereas the variation for other Reynolds number were well above the line. This was the reason that the turbulent boundary layer separation points were not predicted during the computation.

Smith (39) has pointed out the importance of the knowledge of local coefficient of skin friction

mainly due to two reasons. Firstly it is a measure of the velocity gradient at the surface and therefore the stability of the boundary layer and secondly to instigate blade temperature distributions which may be required in the stress analysis of turbine blades. The distribution of heat transfer coefficient is required which, using Reynolds analogy to Ludweig & Tillman the skin friction coefficient is given by

$$C_f = \frac{\tau_w}{\frac{1}{2}\rho U^2} = 0.246\, e^{-1.561\, H}\, Re_\theta^{-0.268} \qquad (4.6)$$

The point ofseparation may therefore be taken as that position where $C_f \simeq 0$.

Figure ( ) shows a comparision between the two criteria used for locating the point of separation based on the above arguments. It is clear from the figure that the criterion $L = -0.2$ indicates early separation for both the cases considered. However when incidence is $-2^\circ$ the differences between thelocation as predicted by the above two different criteria are less . Moreover the nature of the curves are smooth in both the cases.

The final aim of present study was to evaluate the coefficient of drag as suggested by Speidel & Scholz ( 17 ). For this the momentum thickness at the trailing edge on the blade surfaces are

consideration are plotted in figures ( 6E ) (——).
It may be noted that the rate of momentum thickness decrease is more at lower Reynolds number especially on the suction side. Further, on suction side the momentum thickness at trailing edge for $10^{\circ}$ incidence is almost the same as that for $-2^{\circ}$ incidence particularly at lower Reynolds numbers. On pressure surface there is a considerable difference in the above result. It may also be observed that the momentum thickness at trailing edge on pressure surface at incidence $-2^{\circ}$ is more than that at incidence of $10^{\circ}$. The latter result is based on the fact that the boundary layer remained laminar for $10^{\circ}$ incidence on the pressure surface, where as the boundary layer under went transition at 21.5 percent of chord for $-2^{\circ}$ incidence. The former result as discussed above was a bit surprising. It was therefore thought to present the following results in a tabular form to find out the reasons for almost the same momentum thicknesses at the trailing edge for $10^{0}$ and $-2^{0}$ incidences on the suction surface. At a Reynolds number of $10^{4}$ the point of transition for $10^{\circ}$ incidence was at 50 percent chord whereas for $-2^{\circ}$ incidence transition occured at 83.5 percent chord. At first sight it may appear that $(\frac{\theta}{C})$ at trailing edge for $10^{\circ}$ incidence would be much greater than that for $-2^{\circ}$ incidence. From table it appears that

there is not much difference in values of $\theta/C$ at trailing edge for both the incidences, the numerical values being 0.01825 and 0.0165. This may be attributed to the fact that the value of ( $\theta/C$ ) at transition for $-2^{\circ}$ incidences was much greater than ( $\theta/C$ ) at transition , values for $10^{\circ}$ incidence though transition occured much earlier for $10^{\circ}$ incidence. The results at higher Reynolds numbers indicated that there is some difference in the ( $\theta/C$ )T.E value for the two cases of incidences.

Having discussed about the development of momentum thickness at trailing edge on the blade surfaces the last discussion would be about the results of the coefficient of drag calculated for different Reynolds numbers. These results are plotted in figure ( 9 ) along with the results computed by Murali Mohan ( 20 ). The values of $C_D$ as obtained by Squire & Young, for isolated aerofoils, are also given in the same figure. Furthermore the experimental results of M.K.M.M. Swamy (47) as reported by Murali Mohan (20) are also plotted in the above figure. The comparison shows that the computed values of $C_D$ based on the present study are lower than those of Murali Mohan (20) for all the Reynolds numbers. This is because of the fact that the transition was considered to occur much earlier than the position as predicted by Michel's criterion in the present study. Due to this theboundary layer growth at T.E. was more which resulted in higher $C_D$.

The coefficient of drag for $10^{\circ}$ incidence would be higher than that for $-2^{\circ}$ incidence. However the results plotted for the above incidences are reverse in nature. The reason for this is that Michel 's criterion did not predict the point of transition on the pressure surface for $10^{\circ}$ incidence i.e. the boundary layer remain laminar upto the trailing edge for the Reynolds number upto $10^{6}$. The failure of Michal's criterion for the prediction of transition point under such circumstances has already been discussed on page no. . It is therefore apparent that the sum of $\left(\frac{\theta}{C}\right)_{T.S.}$ on suction side and $\left(\frac{\theta}{C}\right)_{T.S.}$ on pfessure side for $10^{\circ}$ incidence side was lower than that of $-2^{\circ}$ incidence. It may be mentioned here that $(\theta/C)_{T.S.}$ on suction side for $10^{\circ}$ incidence is almost equal to $(\theta/C)_{S.S.}$ on the same surface for $-2^{\circ}$ incidence as discussed earlier. The nature of the curve therefore suggests that some other criterion should be used to predict transition on the pressure surfaces for cases under consideration. Under such circumstances the curve of $C_D$ for $10^{\circ}$ incidence would have represented higher values than those of $-2^{\circ}$ incidence. This scheme was not tried in the present study due to the limited time. It is worth mentioning here that thecomputed results based on the present study are in good agreement with the experimental results of K.M.M.Swamy (47). When we compare the present results with the results of Squire & Young theff seems to be

It appears from figure ( 9 ) that when the turbulent boundary layer was separated from the surface, there was an increase in $C_D$ as expected. Murali Mohan (20) has perhaps not shown this aspect in his figure.

## 5. CONCLUSIONS

Viscous flow through compressor cascades has been studied. For this , the experimental results of non - dimensional pressure coefficients for $10^{\circ}$ and $-2^{\circ}$ incidence angles, as reported by Murali Mohan (20) are used as the main data. No artificial transition producing device was used. Laminar boundary layer growth is calculated using the well known Thwaite's method. Michel's criterion has been adopted for the prediction of transition point. It isobserved that the above criterion fails to predict the transition point on pressure surface for $10^{\circ}$ indidence at lower Reynolds numbers . This results in a lower momentum thickness at the blade tfailing edge as compared to when the transition would have occured at some point. The value of H at transition point is assumed to be 1.4.

Turbulent boundary layer calculation is carried out using Truckenbrodt's method.

After predicting the boundary layer growth on the blade surface , Speidel and Scholz method of calculating the coefficient of drag is employed. A lower value of L ( = -0.2 ) is specified for the turbulent boundary layer seperation. This is based on some observavions as reported by Quadir (16) The $C_D$ for $10^{\circ}$ is found to be less than that for $-2^{\circ}$

incidence. This is primarily due to the absence of transition on the pressure surface for $10^{\circ}$ incidence. It is therefore concluded that some other method may be used to predict the transition point under the above circumstances. However the present results are much closer to the experimental results as shown for $-2^{\circ}$ incidence. On comparison with theresults of Squire & Young (which is for isolated aerofoils) it is found that the present computed values of $C_D$ are less as is expected.

The present work may be used to determine the profile losses in an axial flow turbomachine. The omission of the secondary losses and tip clearance losses, should not affect the nature of the loss ve variation with Reynolds number, as they are independent of Reynolds number.

1. WALKER , G.J. "The prediction of boundary layer development on Axial flow turbomachine blades". Conference on Hydraulics and fluid mechanics, 1960. The Instn. of Engineers, Australia.

2. THWAITES, B. "Approximate calculations of the laminar boundary layer" Aeronautical Quarterly, Vol. 1. Pt. Nov. 1949.

3. ROUDBUSH W.H. & SEYMOUR LIEBLEIN "Viscous flow in two dimensional cascades". Chapter 5, N65 23350

4. RALPH H. PENNINGTON "Introductory computer methods and numerical analysis". The Macmillan Company, New York, 1965

5. SAYB , N.J. "The role of boundary layers in axial flow turbomachines and the prediction of their effects".

6. SCHUBAUER , G.B. & SKRAMSTAD " J. Aeronaut Sci. Vol 14, 69 (1947).

7. HINZE , J.O. " Turbulence " McGraw Hill Book Co. 1959.

8. RHODEN , H. " Effects of Reynolds number on the flow through a cascade of Compressor Blades". ARC R and M 2919 (1956)

9. GRANVILLE, P.S. "The calculation of the viscous

10. MICHEL, R. " Etude de la transition sur les profils d'Aile; Establishment d'un point de transition et calcul de la trainee de profil en incompressible". ONERA Report 1/1578 A, July 1961

11. ROSENHEAD , L. ed. "Laminar boundary layers; an account of the development, structure and stability of boundary layers in incompressible fluids together with a description of the associated experimental techniques". Oxford, Clarendon Press, 1963, p.542 .

12. THOMSON B.G.J. "A critical review of existing methods of calculating the turbulent boundary layer". Gt. Britain. Aeronautical resea-rch council, report, 26109, F.M. 3492, Aug 1964.

13. HEAD, M.R. "Entrainment in the turbulent boundary layer". Gt. Britain. Aeronautical resea-rch council, reports and memora-nda, R & M. No. 3152, Sept.1958, London, H.M.S.O., 1960.

14. THOMSON, B.G.J. "The calculation ofshape develop-ment in Incompressible turbulent boundary layers with or without transpiration". North Atlantic Treaty Organisati

developments in boundary layer res -arch, Naples, May, 1965. AGARDOGRAPH, No. 97, pp. 159-90.

15. ROTTA, J.C. "Recent developments in calculation methods for turbulent boundary layers with pressure gradients and heat transfer". Trans. A.S.M.E., Series E, Four. App. Mechanics, Vol.33, No.2, June, 1966, pp. 429-37.

16. QUADIR G.A. "Boundary Layer development on low aspect ratio compressor blading of large camber". Ph.D.Thesis, July1978 Dept. of Mech. Engg. in I.I.Sc Banglore

17. SPANGEL, L. & SCHOLZ, N. "Untersuchungen über die strömungsv -erluste in ebenen Schaufelgittern. VDI - Forschangsheft no. 464, 1957.

18. SCHLICHTING, H. "Boundary Layer Theory" McGraw - Hill Book Company, Inc., New York., 1960.

19. SCHLICHTING H. & SCHOLZ, N. "Über die theoretische berechnung der Strömungsverluste eines ebenev Schaufelgittern". Ingenieur -Archiv, Vol.19, 1951, pp. 42 - 65.

20. MURALI MOHAN V.R. " Technical study of Scale effect in an axial flow fan". A project report of M.E.Course. I.I.Sc Banglore, 1974.

21. HORLOCK , J.H. "Axial flow compressors" Butter Worths Scientific publicat -ions, London, 1958.

22. HORLOCK , J.H. "Axial flow Turbines", Butter Worth, London, 1966.

23. VASANDANI, V.P. "predetermination of the polar diagrams of a profile in plain, stationary turbine and pump cascades". europa - industie - revue Vogal - Verlag, würzburg. nr. 1, March 1959.

24. KLEBANOFF, P.S. TIDSTROM , K.D. & SARGENT, L.M. ( 1962 ). J. Fluid Mech., Vol.12 pp. 1-34

25. SIMONS, H.W. ( 1951) , J. Aeronaut. Sci., Vol. 18, pp. 490 - 498.

26. MORKOVIN, M.V. ( 1969 ) Wright - Patterson Air Force, Base Air Force Flight Dynam. Lab Rep. AFFDL - TR-68-149.

27. WHITE, FRANK M. "Viscous Fluid Flow". 1974, Mc. Graw - Hill, Inc., U.S.A.

28. LIEPMANN, H.W. ( 1943 ) : NACA Wartime Rep. W 107 ( ACR 3H30 )

(1945 ) NACA Wrtime Rep. W87 (ACR4 J28)

29. SCHLICHTING H., & Ulrich, A. ( 1942 ) : Ber. Lilienthal Ges. Luftfahrtforsche, Vol. S10

30. DURHAM J. "Prediction of boundary layer Transition on Turbomachinery Blades".

31. Evans, B.J. " Effects of free - stream turbulence on blade performance in a compressor Cascade". Ph.D.Thesis, Cambridge Univ. 1971.

32. TURNER, A.B. "Local heat transfer measurements on a gas turbine blade", J. Mech. Eng. Sci. Vol.13. No. 1., 1971.

33. APOSTOLOPOULO, "The development of a laminar turbine cascade". M. Engg., thesis, Liverpool Univ. 1965.

34. WILSON D.G. & POPE, J.A. "Conventive heat transfer to gas turbine blade surfaces". Proc. I. Mech. E. Vol. 16, 1954.

35. DURHAM, J. & EDWARDS, J.P. "Heat transfer calculations for turbine blade design". AGARD - CP-73 - 71 paper 2.

36. POLLARD, D. & GOSTELOW, J.P. "Some experiments at low speed on compressor cascades." Trans. A.S.M.E. (A) vol. p.427,1967

37. WALKER, G.J. "An investigation of boundary layer transition on an axial flow compressor blade". Australian ARL ME Report 122 July 1968.

38. COLE, D.E. & Hirst, E.A. " (1968 ) : Proc. Comput. Turbul. Boundary layers, Vol-II, Department of Mech. Engg. , Stanford University, Stanford, Calif.

39 - on last page

40. STRATFORD B.S. The prediction of separation of the turbulent boundary layer". J. Fluid Mech. , Vol. 5., part I, 1959, pp. 1-16.

41. MASKELL, E.C. "Approximate calculation of the turbulent boundary layer in two dimensional incompressible flow". A.R.C. 14 654, November 1951.

42. THWAITES , B "Incompressible Aerodynamic". Oxford at the clarendon press, 1960.

43. BOBE, G.O.M. " M. Phil Thesis, University of Edinburgh, 1973.

44. HALL , D.J. & GIBBINGS, J.C. " Influence of stream turbulence and pressure gradient upon boundary layer transition". J. Mech. Engg. Science, Vol 14. No. 2, 1972.

45. CRABTREE, L.F. " The formation of regions of separated flow on wing surfaces". Aeronaut Res. Count. Rep. memo. Memo. 3122, 1959.

46. SMITH, A.M.O. & CAMBERONI, N. "Transition, pressure gradient and stability theory; Proc. 9th Int. Congr. Appl. Mech. 1956.

47. K.M.Mruthunjaya

47. K.M.MRUTHUNJAYA SWAMY — " Flow investigation in a cooling tower fan". Project , Report for M.E. in Mech. Engg. I.I.Sc. Banglore.

46. HORTON, H.P. — " A semi-empirical theory for the growth and bursting of laminar seperation bubbles."
ARC C.P. 1073, June 1967.

39. SMITH, D.J.L. — "Turbulent Boundary Layer Theory and its Application to Profile Design"
ARC C.P. No. 868. March, 1965

Table I. RESULTS IN BRIEF
(For Suction Side)

| Blade or | Angle of Incidence | Transition Point ( $x_{tr}/c$ ) | Momentum Thickness ($\theta/c$) at Transition | Momentum Thickness ($\theta/c$) at Trailing Edge |
|---|---|---|---|---|
| B4 | 10° | 0.670 | 0.3165 E-1 | 0.0546 |
| | -2° | 0.930 | 0.4377 E-1 | 0.0563 |
| B4 | 10° | 0.565 | 0.1159 E-1 | 0.0250 |
| | -2° | 0.870 | 0.1562 E-1 | 0.0252 |
| B5 | 10° | 0.500 | 0.7106 E-2 | 0.0182 |
| | -2° | 0.835 | 0.9909 E-2 | 0.0185 |
| B5 | 10° | 0.340 | 0.2170 E-2 | 0.0096 |
| | -2° | 0.750 | 0.3445 E-2 | 0.0085 |
| B6 | 10° | 0.260 | 0.1071 E-2 | 0.0077 |
| | -2° | 0.700 | 0.2178 E-2 | 0.0065 |
| B6 | 10° | 0.160 | 0.3704 E-3 | 0.0055 |
| | -2° | 0.575 | 0.7328 E-3 | 0.0040 |
| B7 | 10° | 0.125 | 0.2161 E-3 | 0.0049 |
| | -2° | 0.500 | 0.4487 E-3 | 0.0035 |
| B7 | 10° | 0.095 | 0.7191 E-4 | 0.0038 |
| | -2° | 0.290 | 0.1317 E-3 | 0.0034 |
| B8 | 10° | 0.080 | 0.4219 E-4 | 0.0035 |
| | -2° | 0.200 | 0.7489 E-4 | 0.0035 |
| B8 | 10° | 0.060 | 0.1437 E-4 | 0.0027 |
| | -2° | 0.090 | 0.2048 E-4 | 0.0032 |
| B9 | 10° | 0.050 | 0.8648 E-5 | 0.0025 |
| | -2° | 0.070 | 0.1213 E-4 | 0.0030 |

Table II. RESULTS IN BRIEF
(For Pressure Side)

| Reynolds Number | Angle of Incidence | Transition Point ($x_{tr}/c$) | Momentum Thickness ($\theta/c$) at Transition | Momentum Thickness ($\theta/c$) at Trailing Ed |
|---|---|---|---|---|
| 1 E4 | 10° | ——— | 0.1800 E-1 | 0.0210 |
| | -2° | ——— | 0.1513 E-1 | 0.0295 |
| 5 E4 | 10° | ——— | 0.8051 E -2 | 0.0093 |
| | -2° | ——— | 0.6765 E-2 | 0.0132 |
| 1 E5 | 10° | ——— | 0.5693 E-2 | 0.0065 |
| | -2° | ——— | 0.4783 E-2 | 0.0092 |
| 5 E5 | 10° | ——— | 0.2546 E-2 | 0.0030 |
| | -2° | ——— | 0.2139 E-2 | 0.0043 |
| 1 E6 | 10° | ——— | 0.1803 E-2 | 0.0022 |
| | -2° | 0.675 | 0.2530 E-2 | 0.0034 |
| 5 E6 | 10° | ——— | 0.8051 E-3 | 0.0012 |
| | -2° | 0.360 | 0.7223 E-3 | 0.0025 |
| 1 E7 | 10° | ——— | 0.5693 E-3 | 0.0010 |
| | -2° | 0.280 | 0.4214 E-3 | 0.0023 |
| 5 E7 | 10° | 0.500 | 0.2144 E-3 | 0.0010 |
| | -2° | 0.165 | 0.1242 E-3 | 0.0019 |
| 1 E8 | 10° | 0.385 | 0.1258 E-3 | 0.0009 |
| | -2° | 0.135 | 0.7508 E-4 | 0.0017 |
| 5 E8 | 10° | 0.170 | 0.3481 E-4 | 0.0008 |
| | -2° | 0.080 | 0.2165 E-4 | 0.0015 |
| 1 E9 | 10° | 0.135 | 0.2101 E-4 | 0.0008 |
| | -2° | 0.070 | 0.1275 E-4 | 0.0013 |

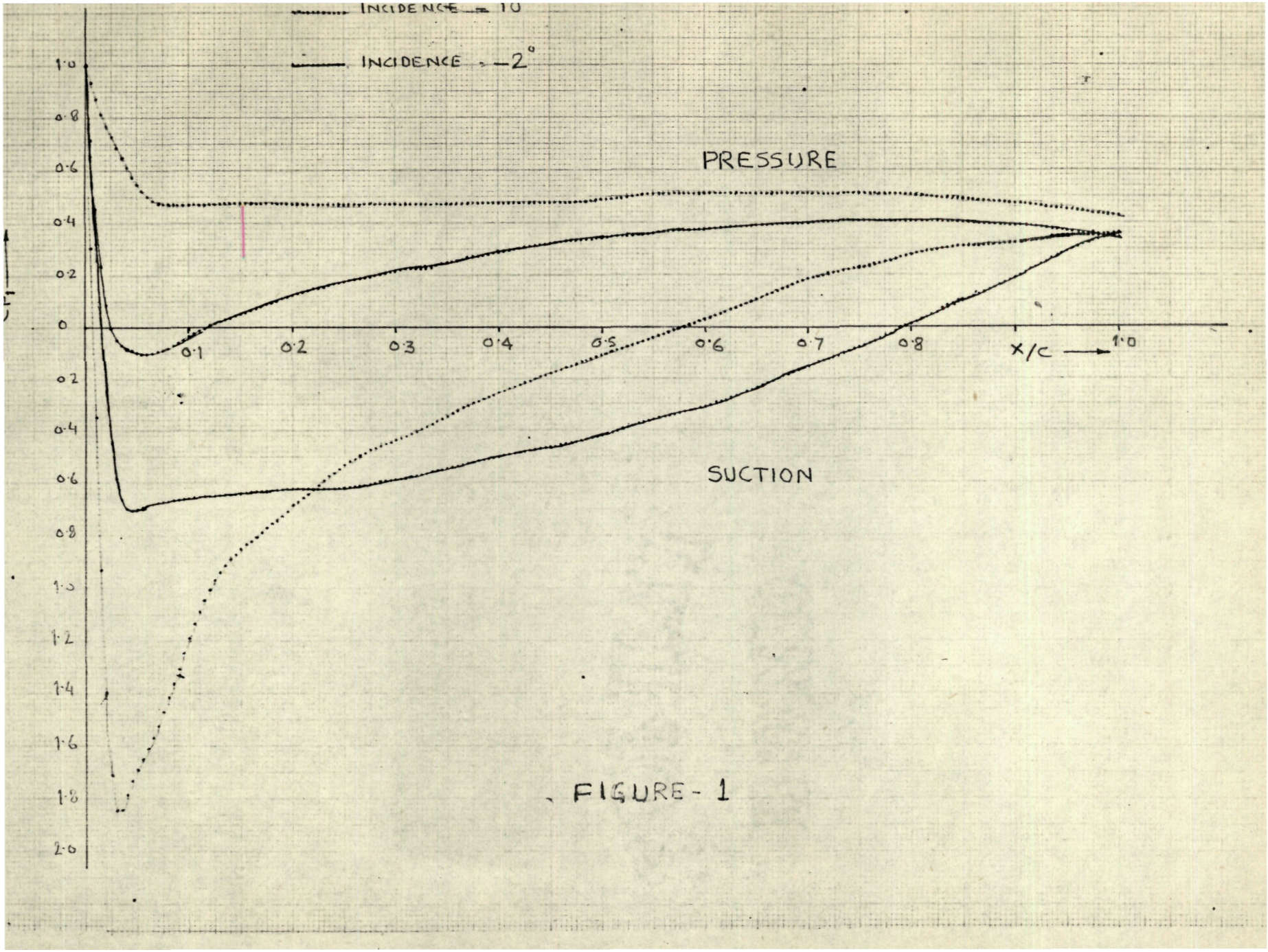
INCIDENCE = 10°
INCIDENCE = −2°
PRESSURE
SUCTION
X/C
1·0
0·8
0·6
0·4
0·2
0
0·1
0·2
0·3
0·4
0·5
0·6
0·7
0·8
1·0
1·2
1·4
1·6
1·8
2·0

FIGURE - 1

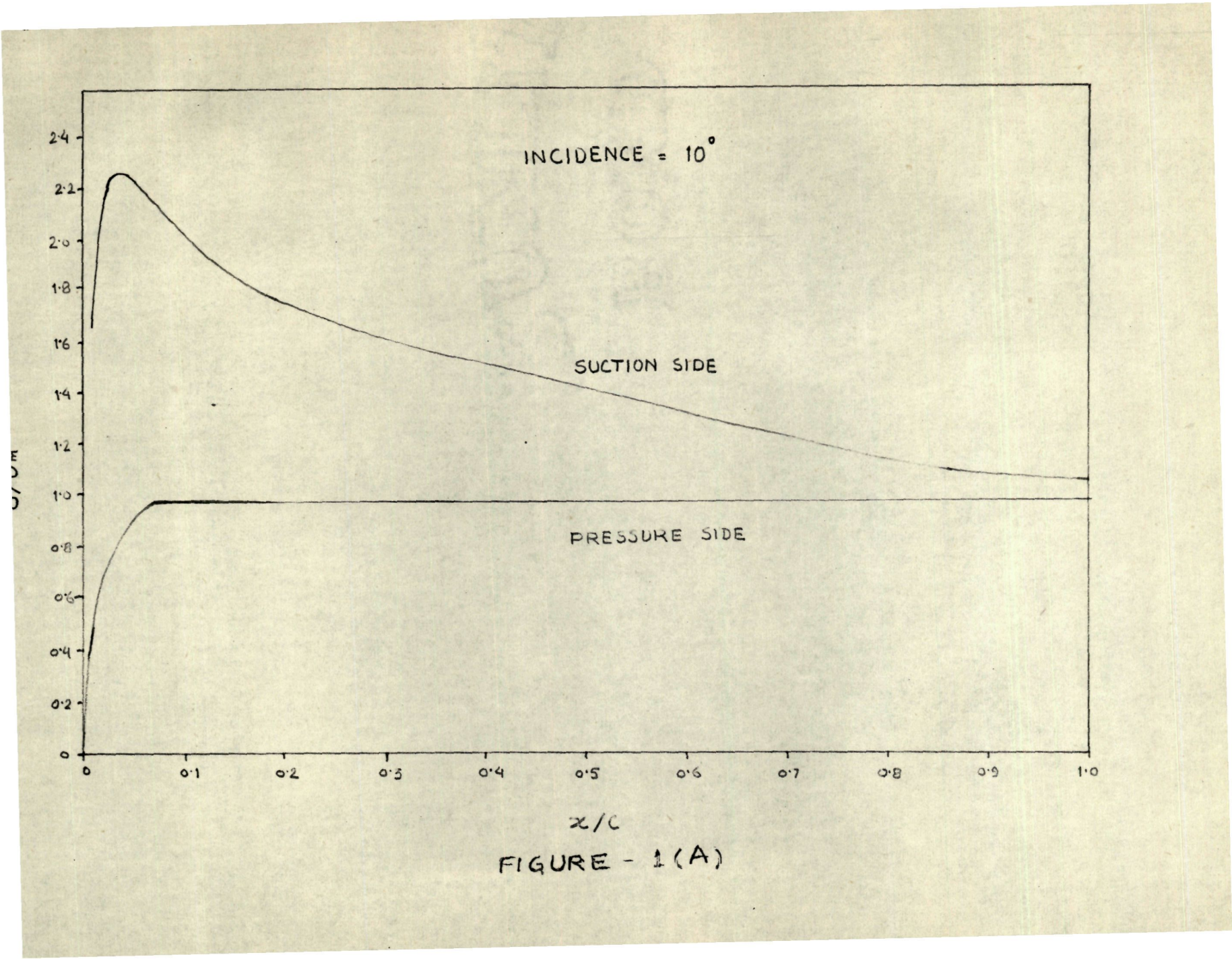
INCIDENCE = 10°
SUCTION SIDE
PRESSURE SIDE
2·4
2·2
2·0
1·8
1·6
1·4
1·2
1·0
0·8
0·6
0·4
0·2
0
0
0·1
0·2
0·3
0·4
0·5
0·6
0·7
0·8
0·9
1·0
x/c

FIGURE - 1(A)

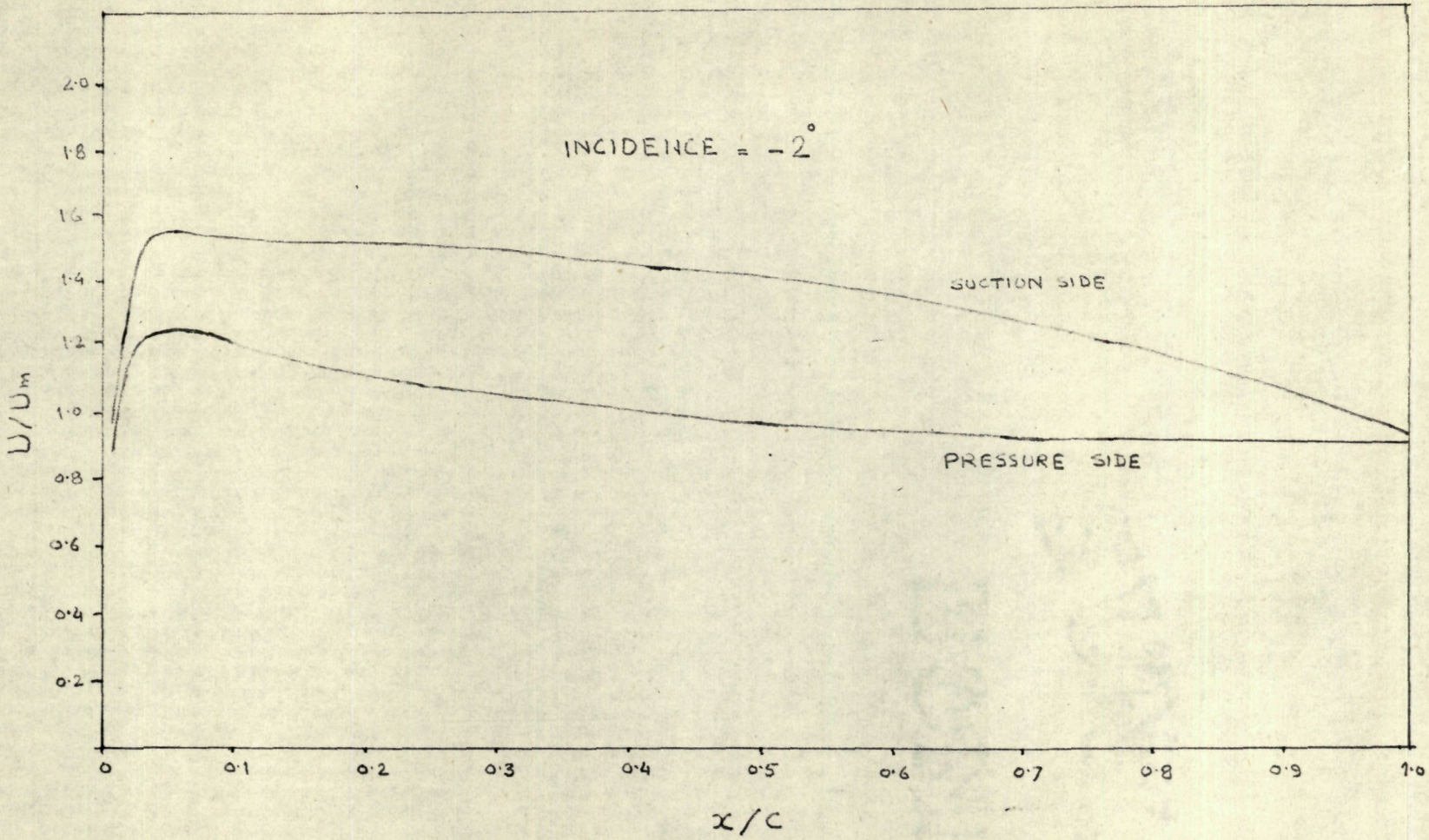
INCIDENCE = −2°
SUCTION SIDE
PRESSURE SIDE
U/Um
2·0
1·8
1·6
1·4
1·2
1·0
0·8
0·6
0·4
0·2
0
0·1
0·2
0·3
0·4
0·5
0·6
0·7
0·8
0·9
1·0
x/c

FIGURE - 1 (B)

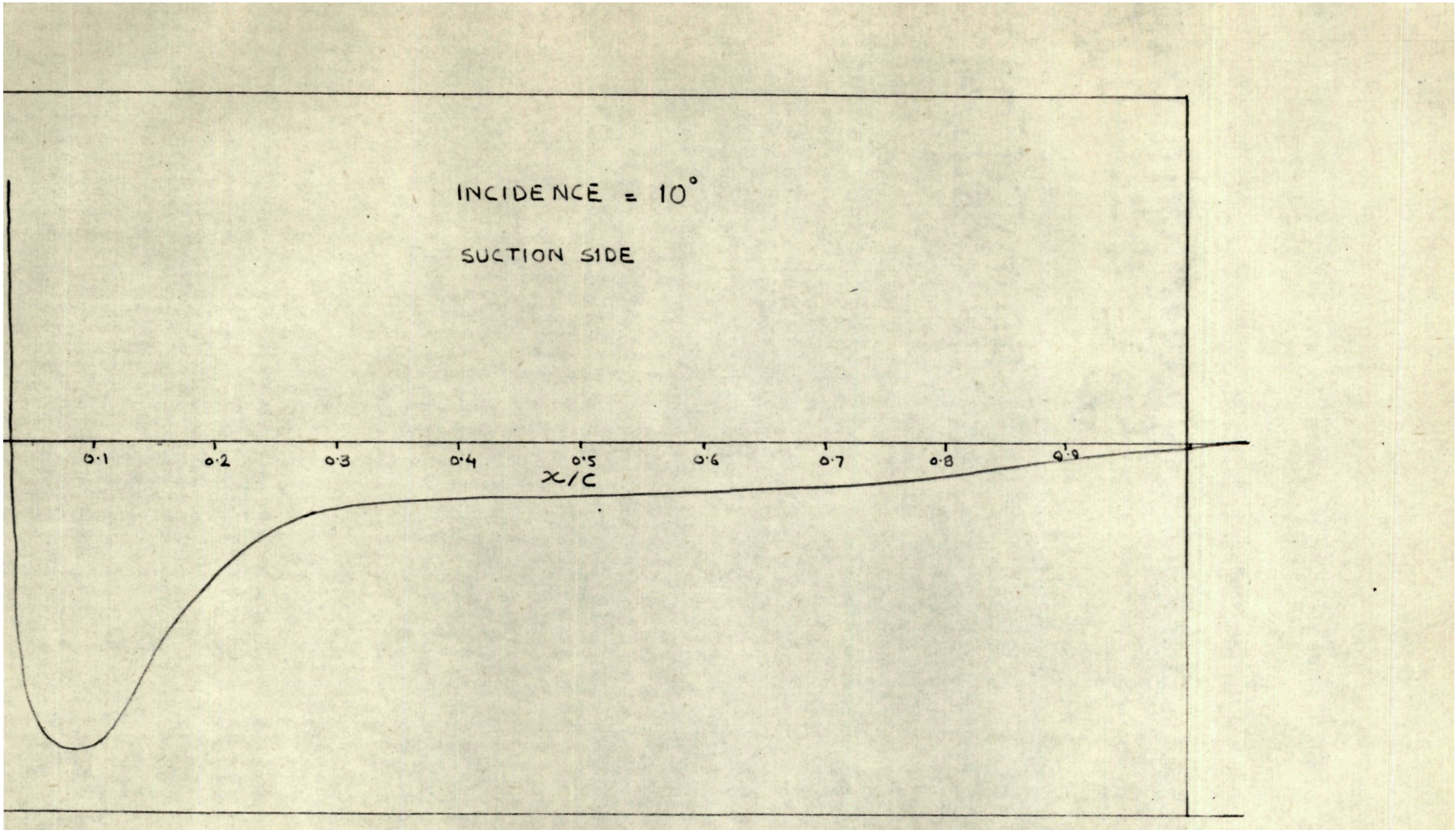


FIGURE - 2 (A)

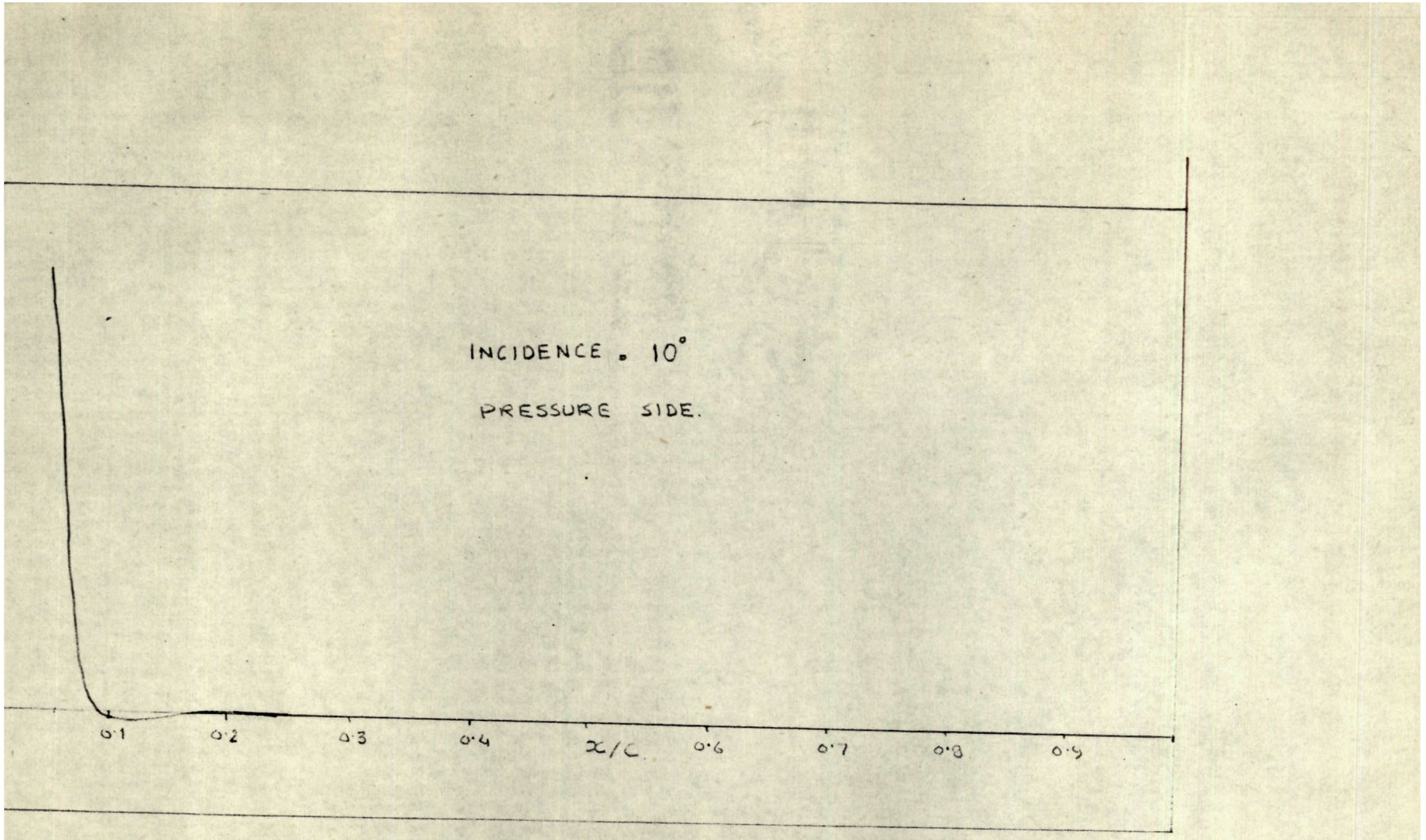


FIGURE - 2 (B)

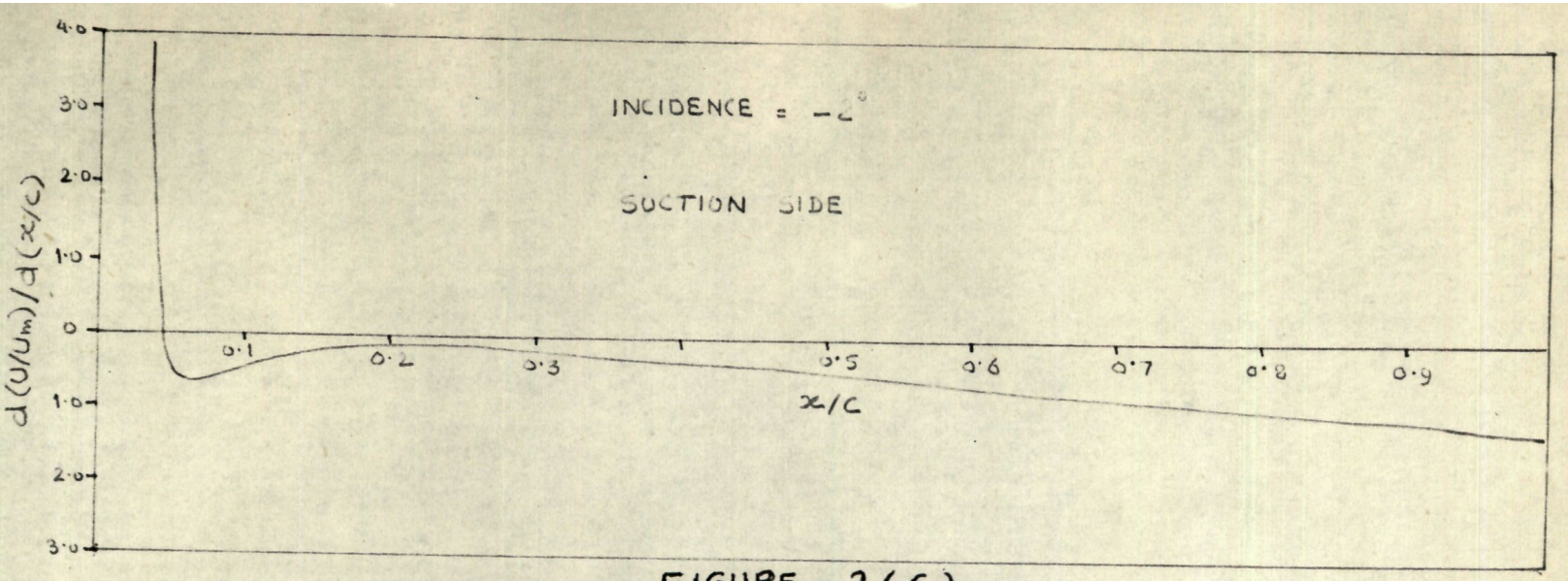


FIGURE - 2(C)

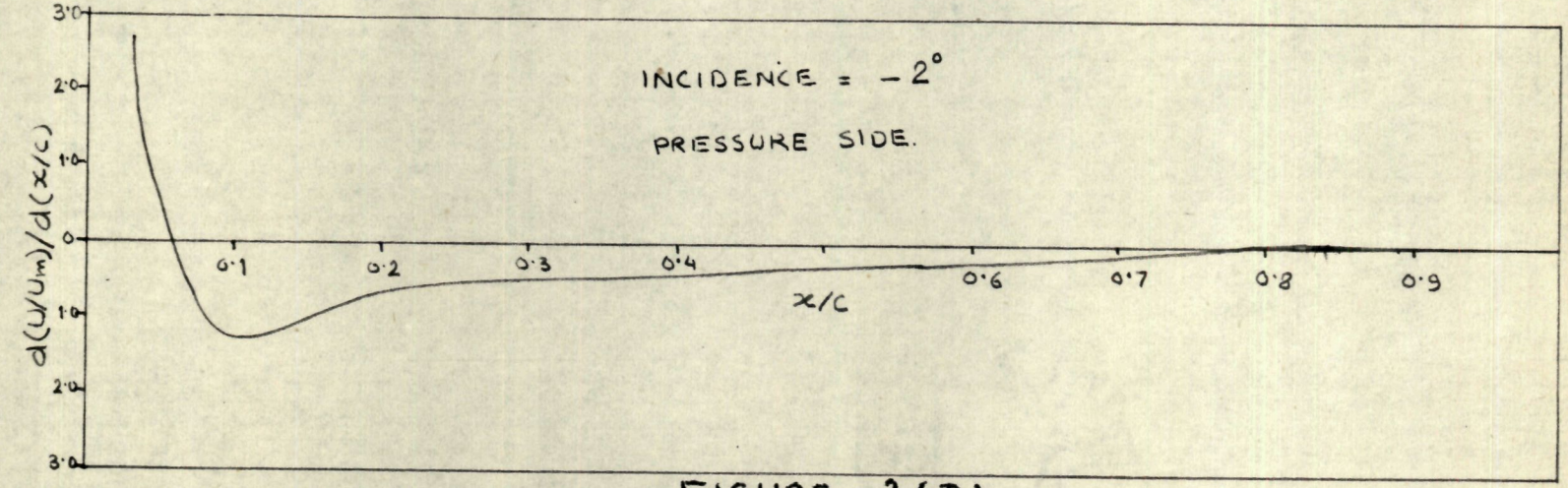


FIGURE - 2(D)

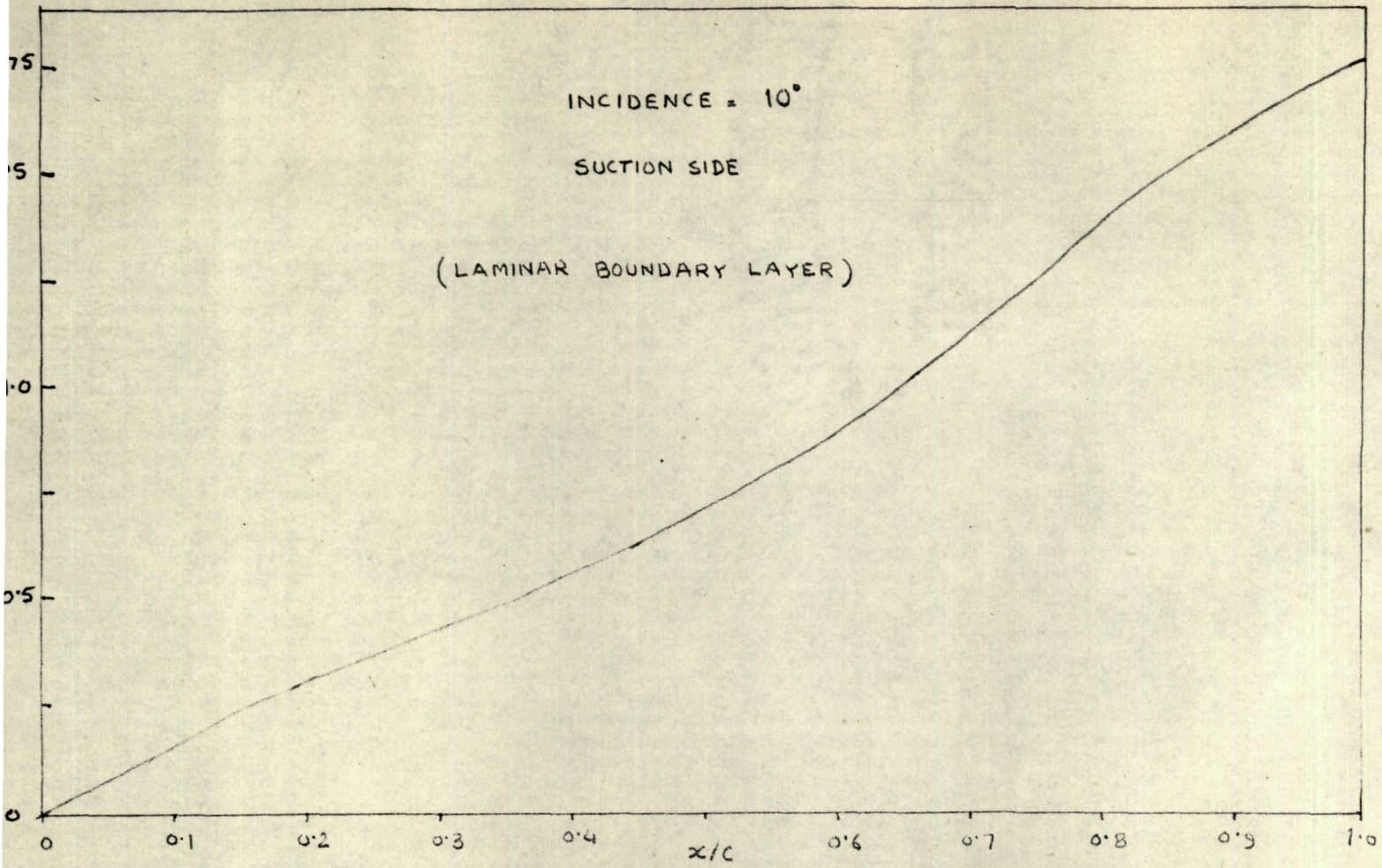
INCIDENCE = 10°
SUCTION SIDE
(LAMINAR BOUNDARY LAYER)
0
0·1
0·2
0·3
0·4
x/c
0·6
0·7
0·8
0·9
1·0

FIGURE - 3(A)

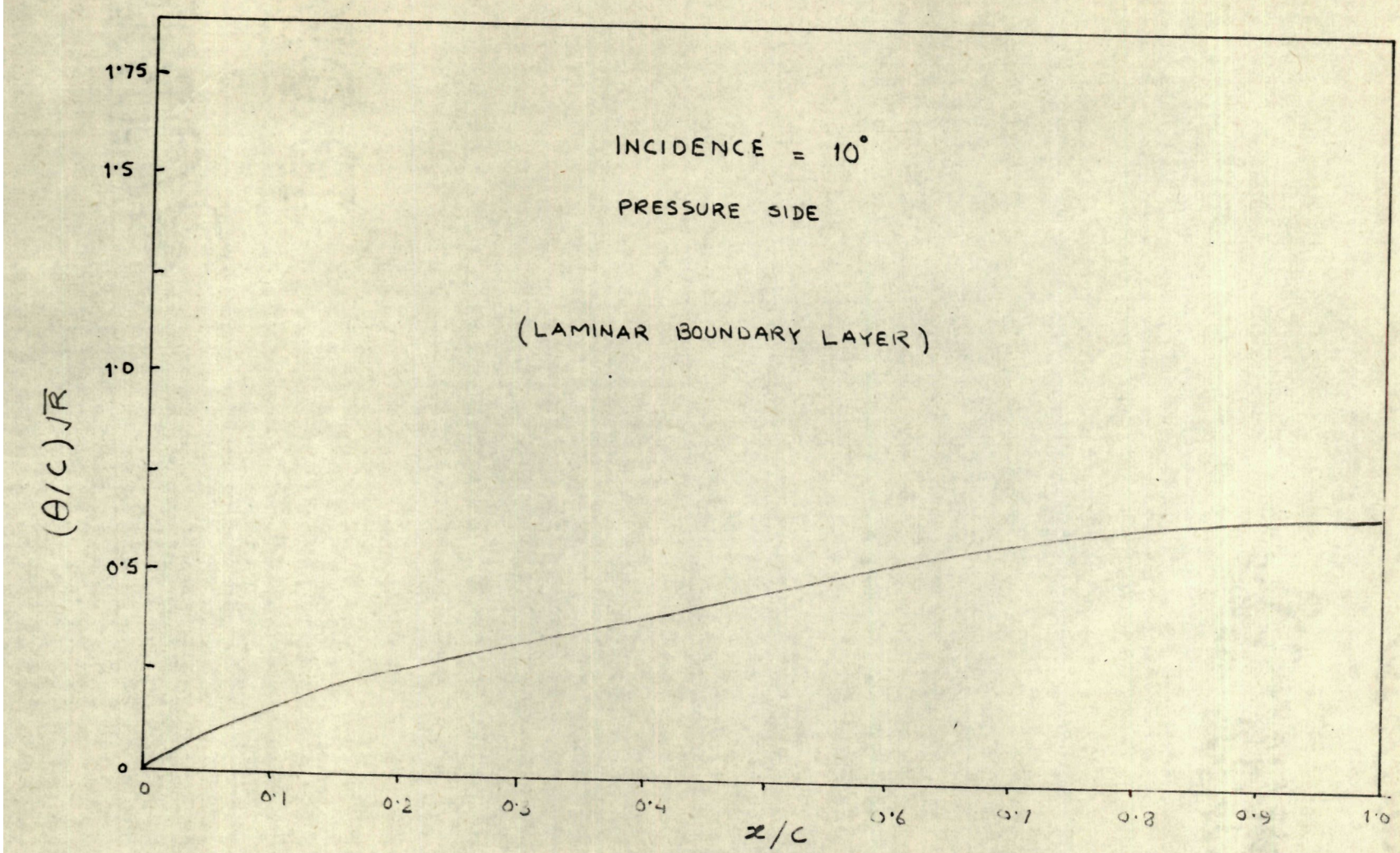
INCIDENCE = 10°
PRESSURE SIDE
(LAMINAR BOUNDARY LAYER)
(θ/c)√R
1·75
1·5
1·0
0·5
0
0
0·1
0·2
0·3
0·4
0·6
0·7
0·8
0·9
1·0
x/c

FIGURE- 3(B)

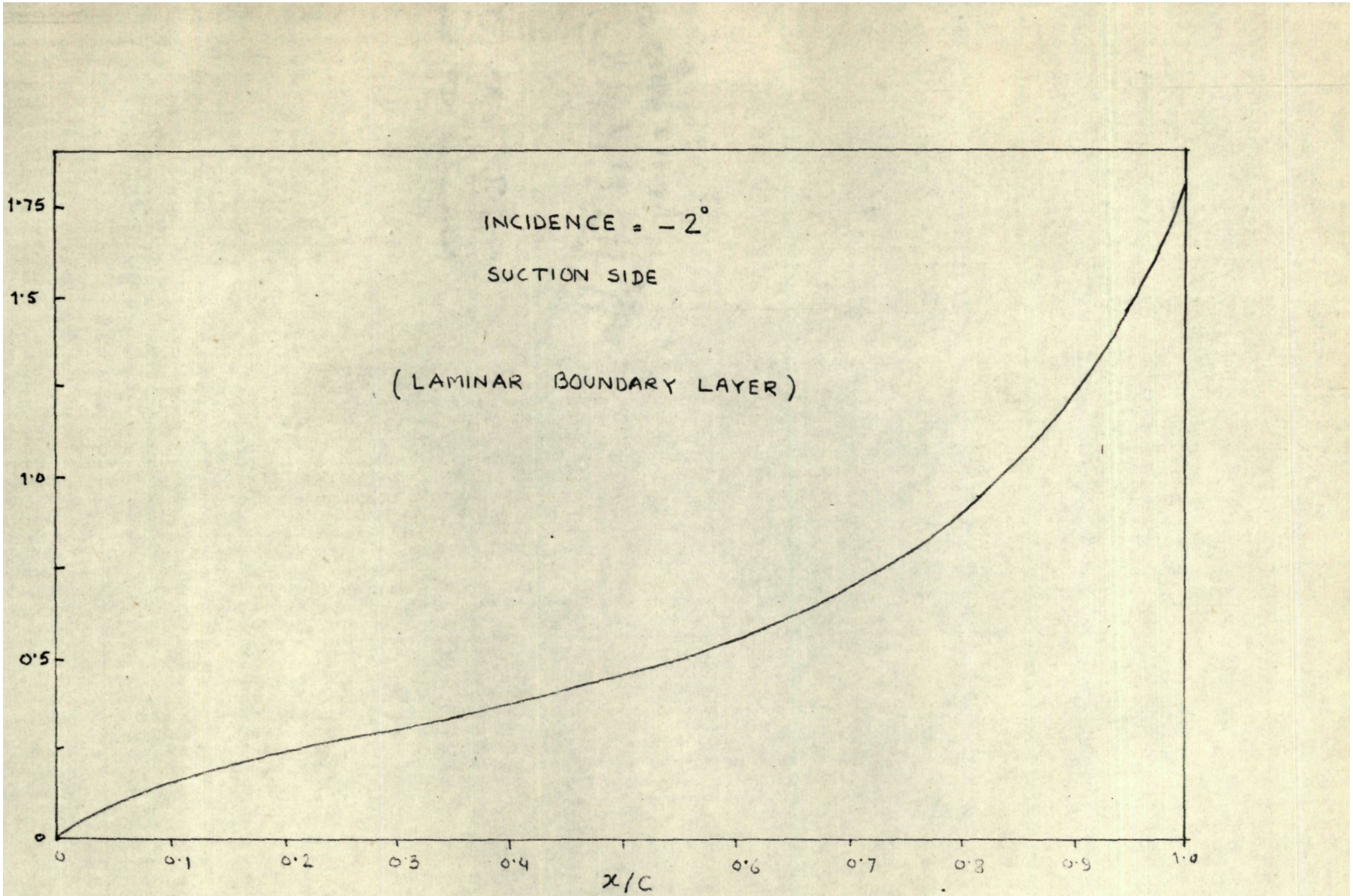
INCIDENCE = −2°
SUCTION SIDE
(LAMINAR BOUNDARY LAYER)
1·75
1·5
1·0
0·5
0
0
0·1
0·2
0·3
0·4
0·6
0·7
0·8
0·9
1·0
x/C

FIGURE - 3(C)

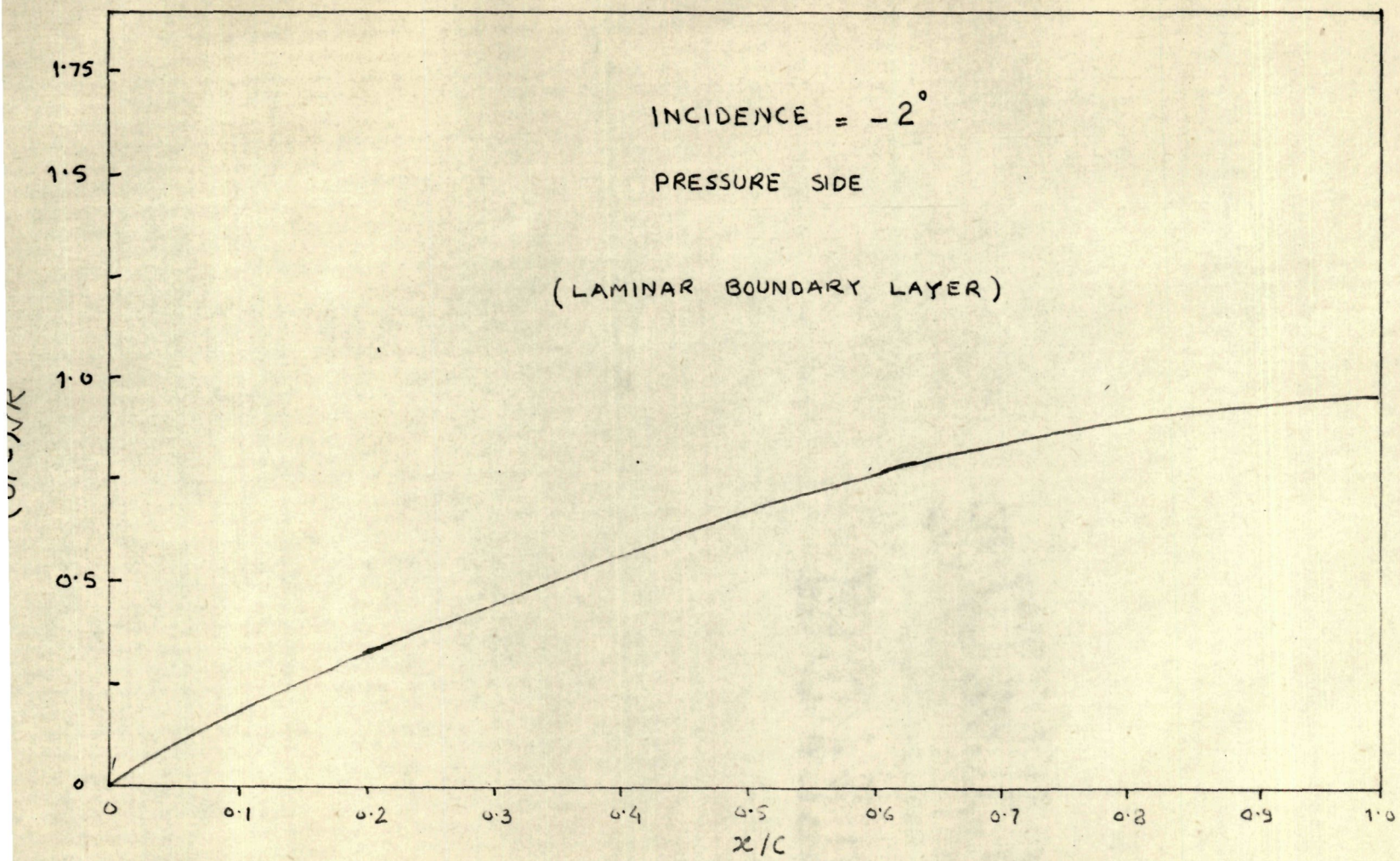
INCIDENCE = −2°
PRESSURE SIDE
(LAMINAR BOUNDARY LAYER)
1·75
1·5
1·0
0·5
0
0
0·1
0·2
0·3
0·4
0·5
0·6
0·7
0·8
0·9
1·0
x/c

FIGURE - 3(D)

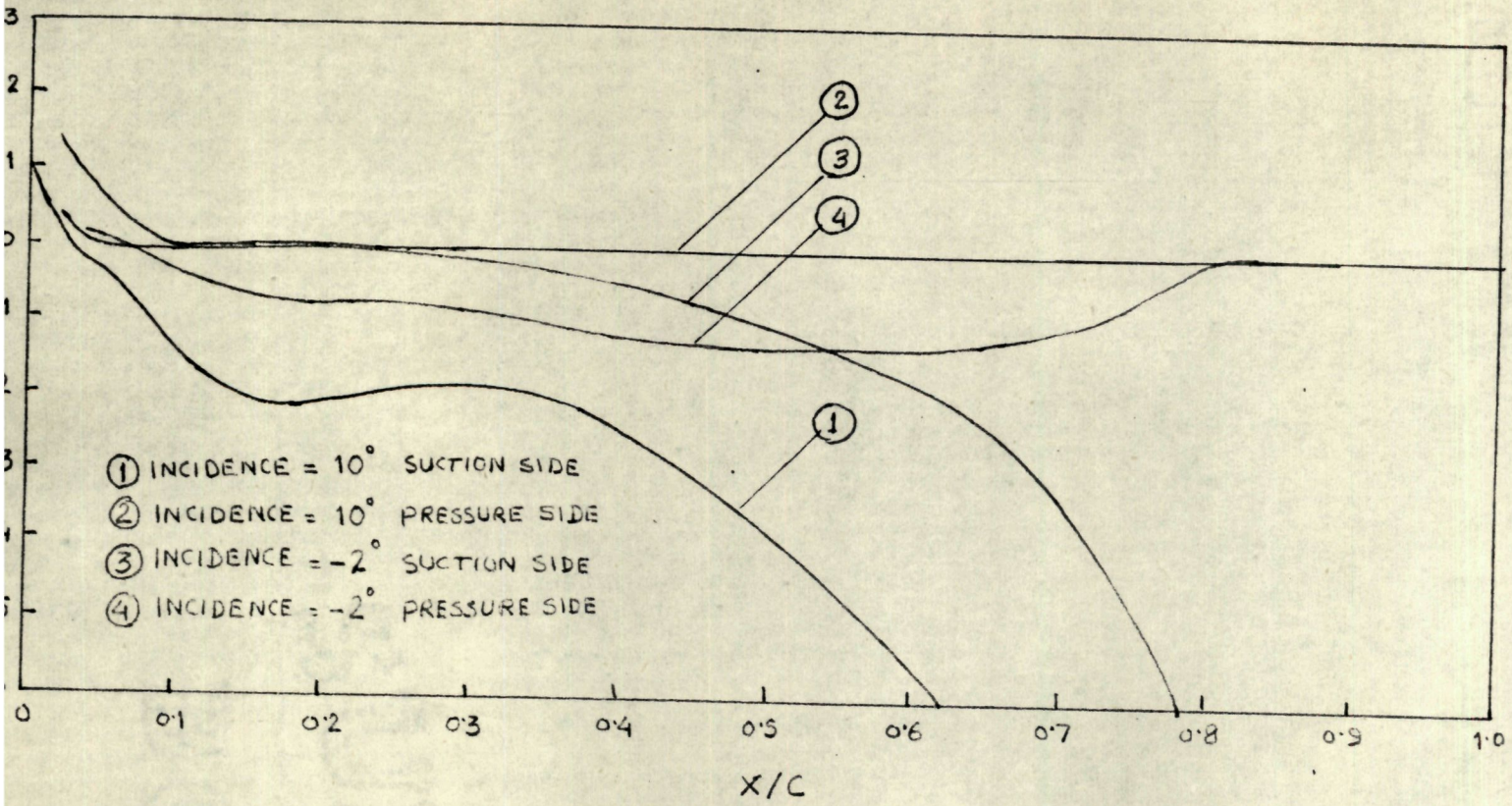
3
2
1
0
1
2
3
4
2
3
4
1
① INCIDENCE = 10° SUCTION SIDE
② INCIDENCE = 10° PRESSURE SIDE
③ INCIDENCE = -2° SUCTION SIDE
④ INCIDENCE = -2° PRESSURE SIDE
0
0·1
0·2
0·3
0·4
0·5
0·6
0·7
0·8
0·9
1·0
X/C

FIGURE - 4

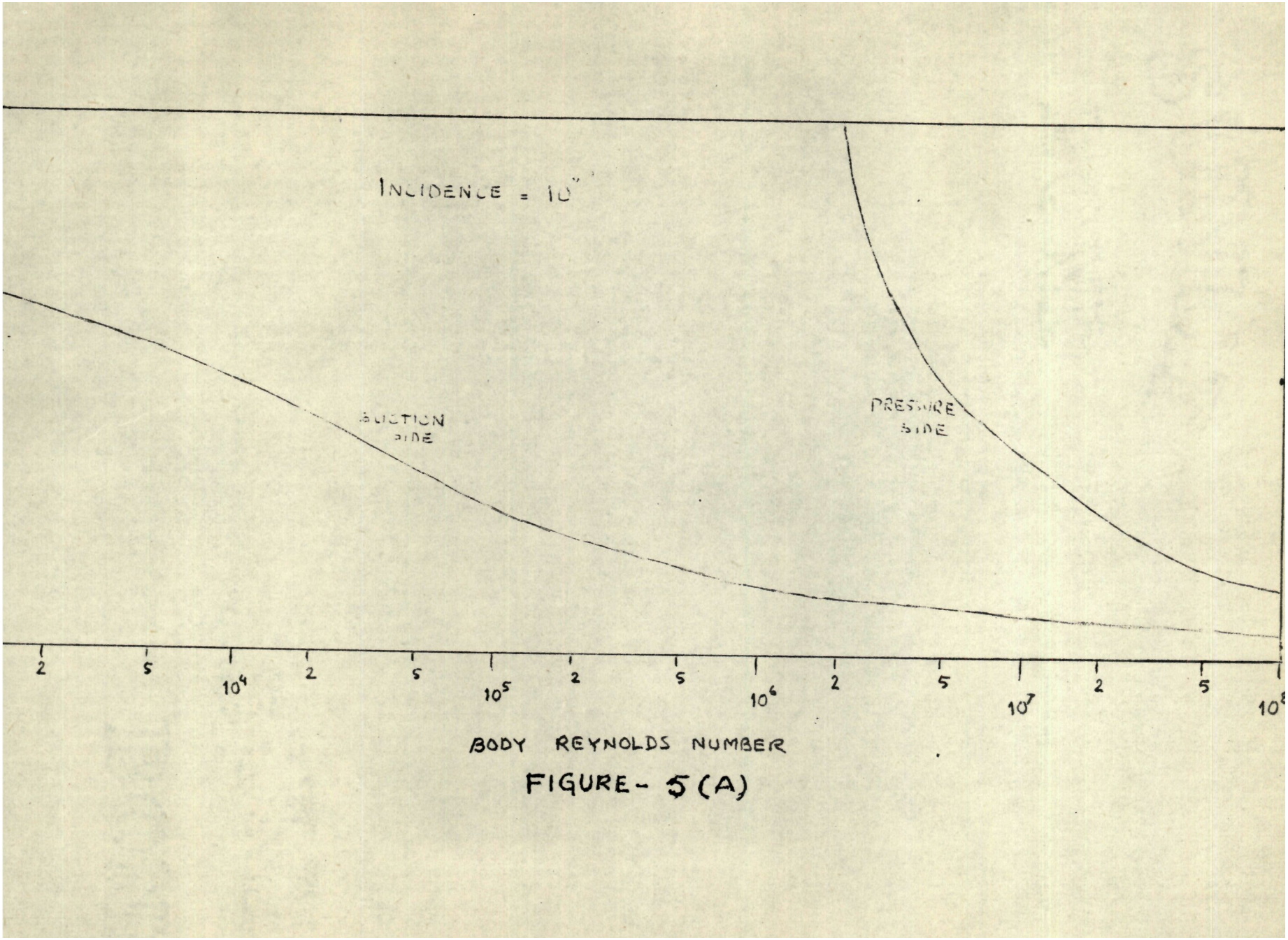
INCIDENCE = 10°
SUCTION SIDE
PRESSURE SIDE
2
5
10⁴
2
5
10⁵
2
5
10⁶
2
5
10⁷
2
5
BODY REYNOLDS NUMBER

FIGURE - 5 (A)

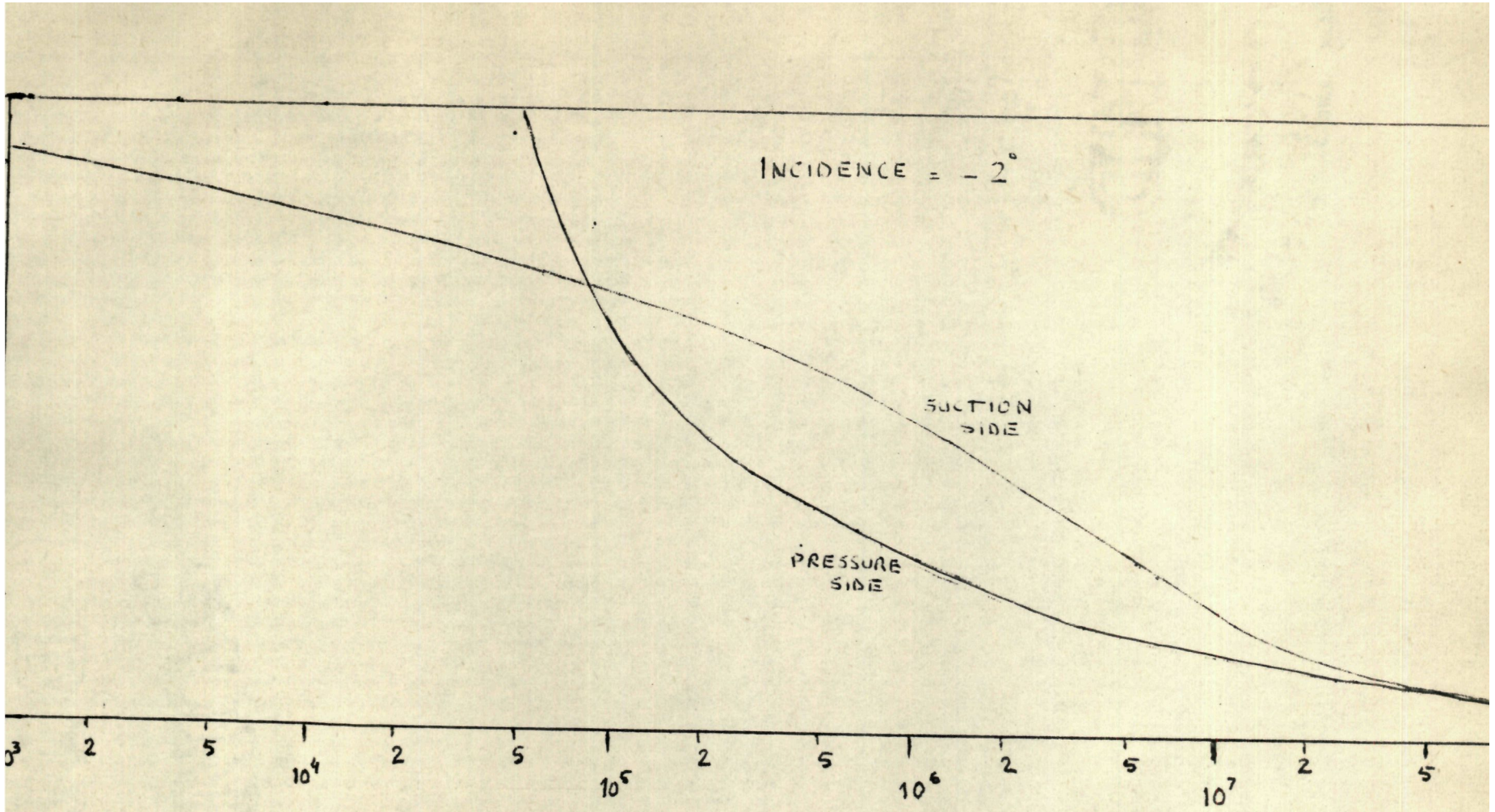
INCIDENCE = - 2°
SUCTION SIDE
PRESSURE SIDE
2
5
10⁴
2
5
10⁵
2
5
10⁶
2
5
10⁷
2
5
BODY REYNOLDS NUMBER

FIGURE - 5 (B)

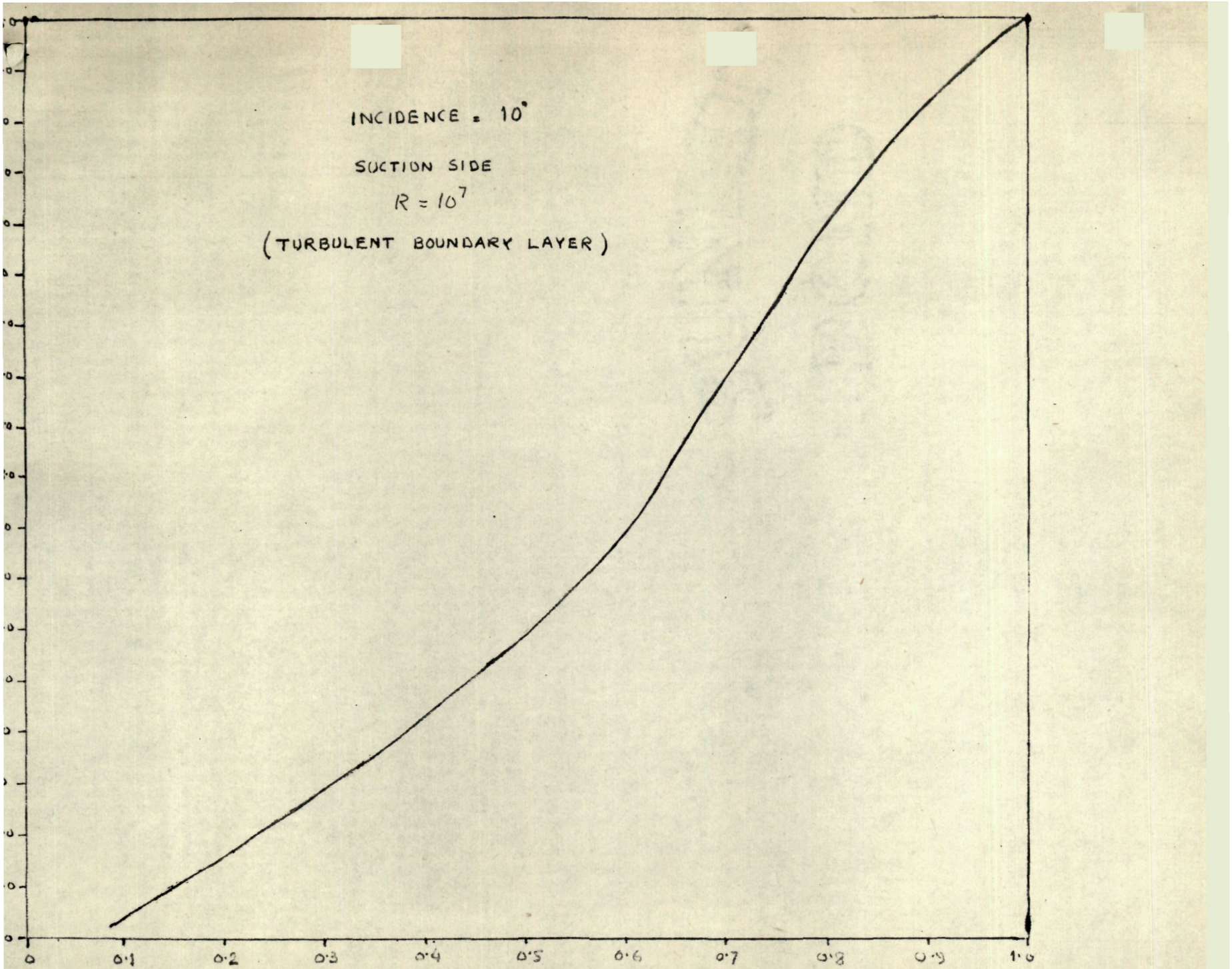
INCIDENCE = 10°
SUCTION SIDE
R = 10^7
(TURBULENT BOUNDARY LAYER)
0
0·1
0·2
0·3
0·4
0·5
0·6
0·7
0·8
0·9
1·0
x/c

FIGURE - 6(A)

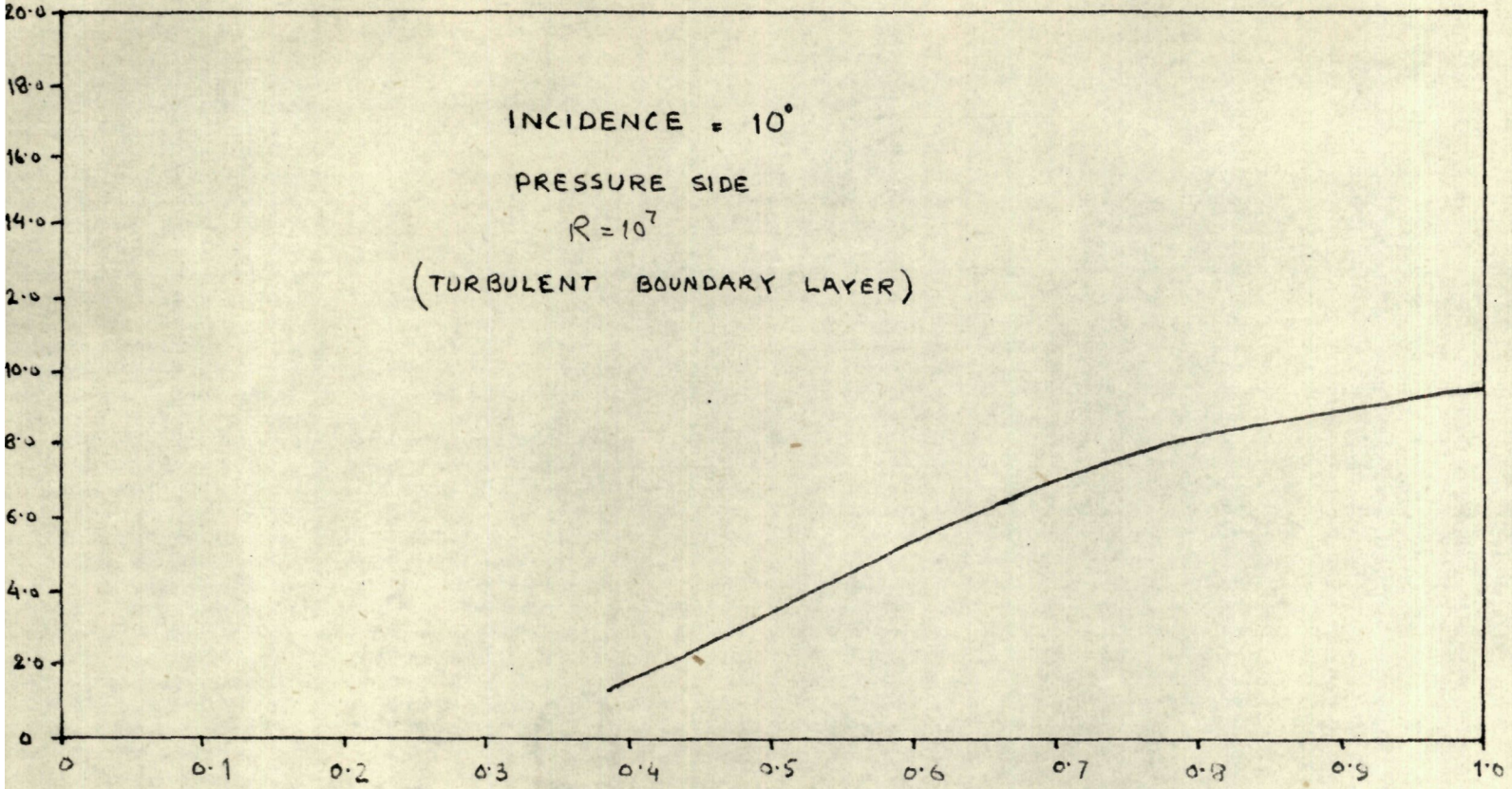
INCIDENCE = 10°
PRESSURE SIDE
R = 10^7
(TURBULENT BOUNDARY LAYER)
20·0
18·0
16·0
14·0
12·0
10·0
8·0
6·0
4·0
2·0
0
0
0·1
0·2
0·3
0·4
0·5
0·6
0·7
0·8
0·9
1·0
x/c

FIGURE- 6 (B)

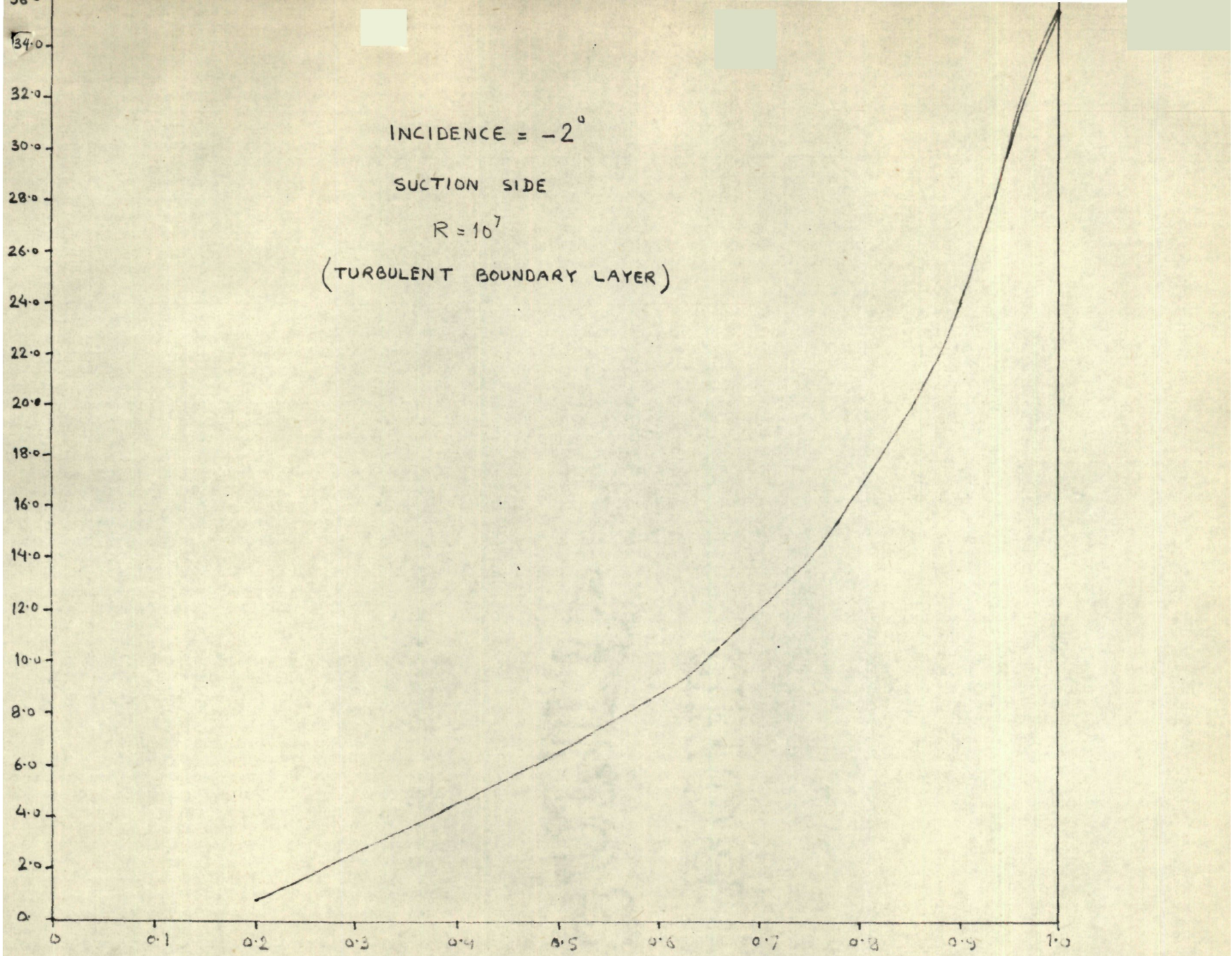
INCIDENCE = −2°
SUCTION SIDE
R = 10^7
(TURBULENT BOUNDARY LAYER)
34·0
32·0
30·0
28·0
26·0
24·0
22·0
20·0
18·0
16·0
14·0
12·0
10·0
8·0
6·0
4·0
2·0
0
0·1
0·2
0·3
0·4
0·5
0·6
0·7
0·8
0·9
1·0
x/c

FIGURE - 6(C)

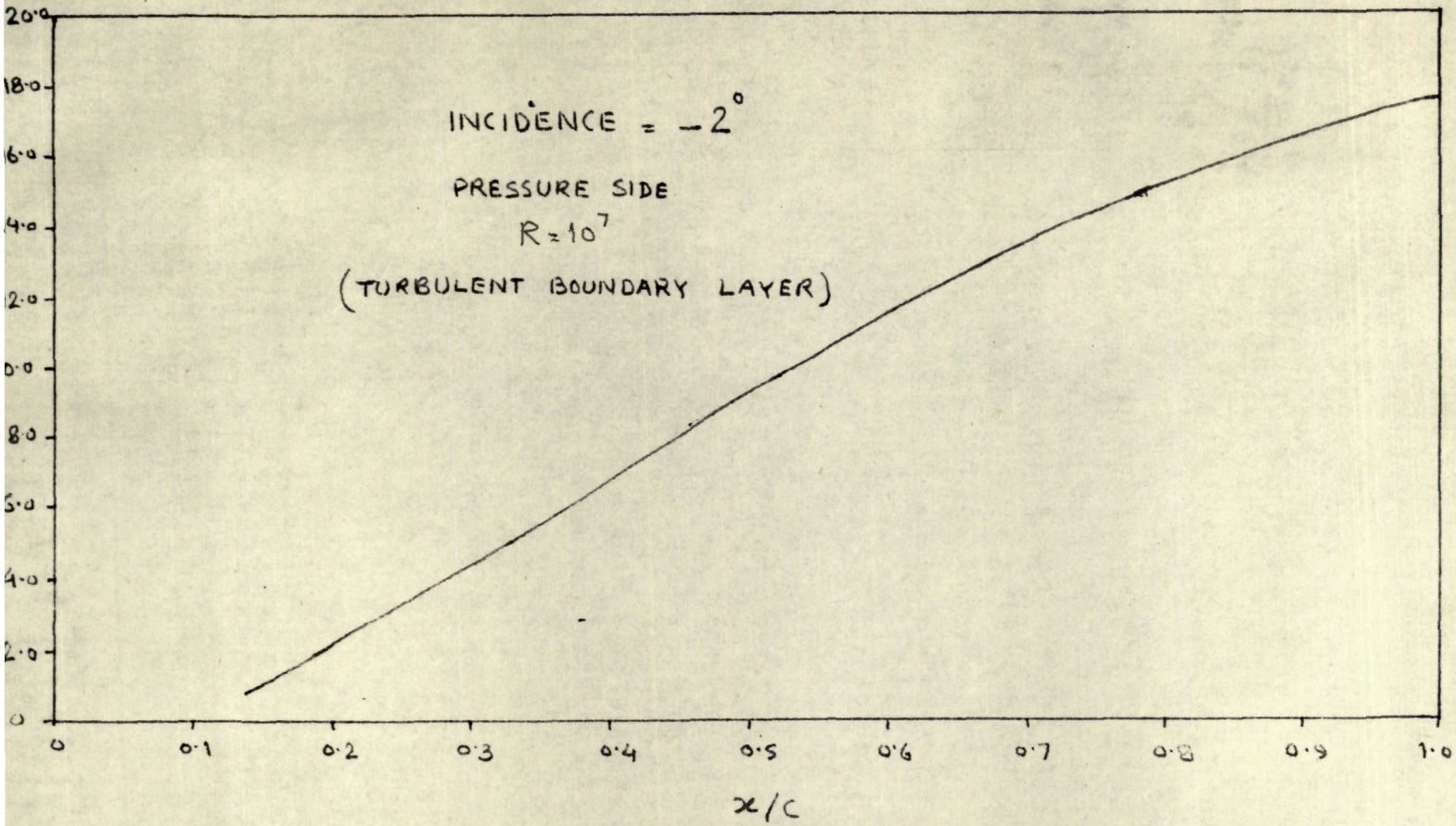
INCIDENCE = −2°
PRESSURE SIDE
R = 10^7
(TURBULENT BOUNDARY LAYER)
20·0
18·0
16·0
14·0
12·0
10·0
8·0
6·0
4·0
2·0
0
0
0·1
0·2
0·3
0·4
0·5
0·6
0·7
0·8
0·9
1·0
x/c

FIGURE - 6(D)

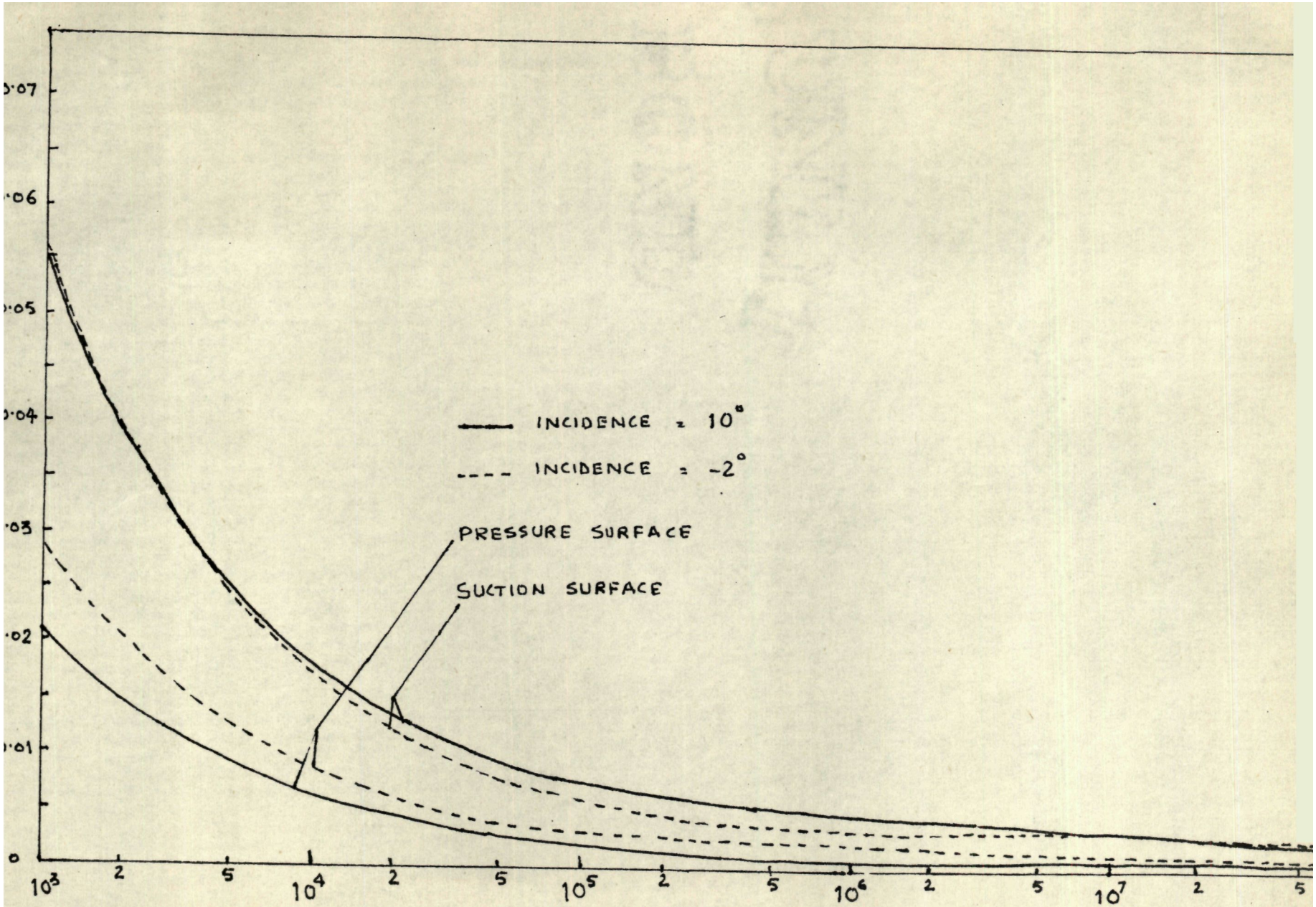
·07
·06
·05
·04
·03
·02
·01
0
INCIDENCE = 10°
INCIDENCE = -2°
PRESSURE SURFACE
SUCTION SURFACE
10³
2
5
10⁴
2
5
10⁵
2
5
10⁶
2
5
10⁷
2
5
BODY REYNOLDS NUMBER

FIGURE-6(E)

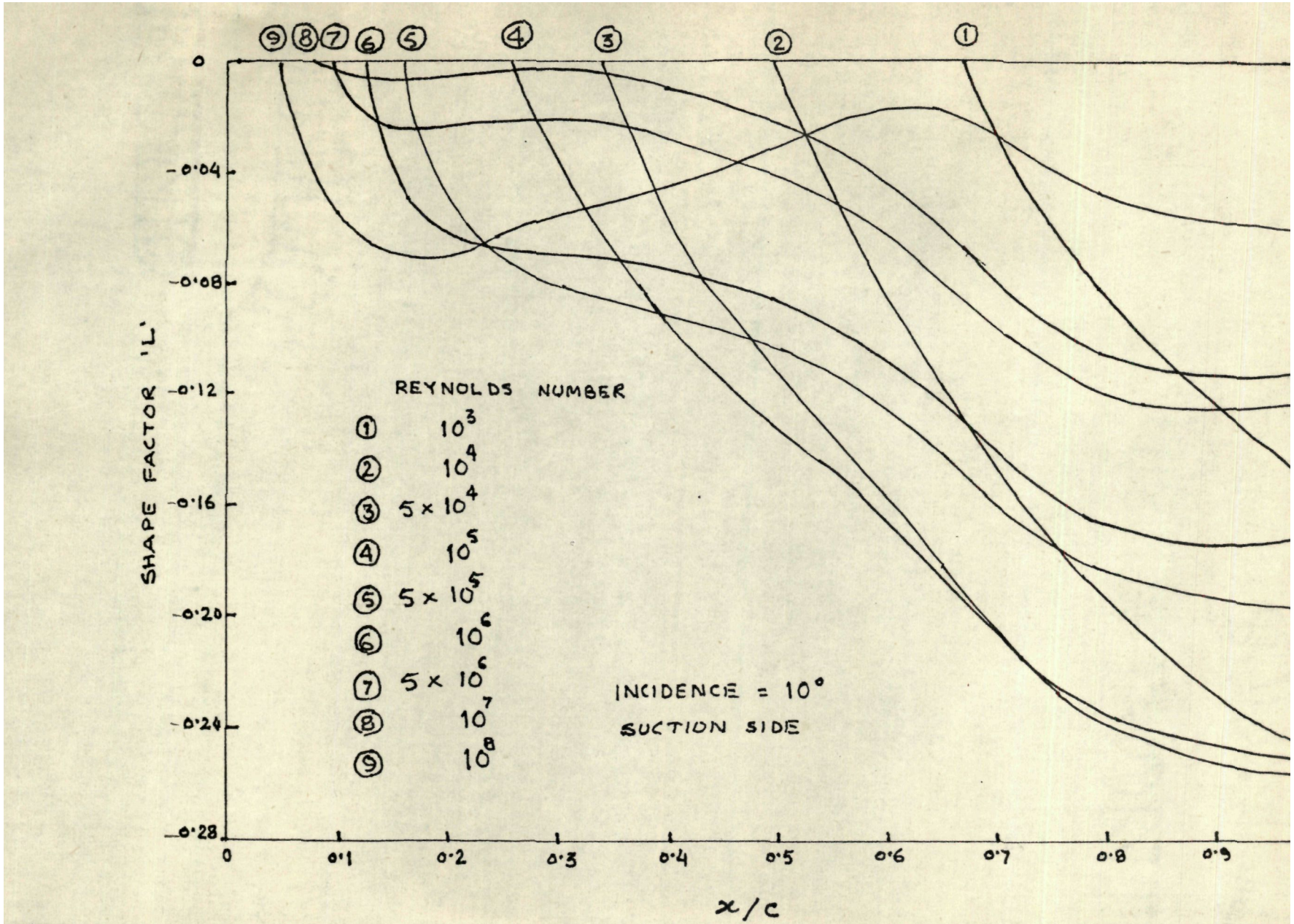
⑨ ⑧ ⑦ ⑥ ⑤ ④ ③ ② ①
0
-0·04
-0·08
-0·12
-0·16
-0·20
-0·24
-0·28
SHAPE FACTOR 'L'
REYNOLDS NUMBER
① $10^3$
② $10^4$
③ $5 \times 10^4$
④ $10^5$
⑤ $5 \times 10^5$
⑥ $10^6$
⑦ $5 \times 10^6$
⑧ $10^7$
⑨ $10^8$
INCIDENCE = 10°
SUCTION SIDE
0
0·1
0·2
0·3
0·4
0·5
0·6
0·7
0·8
0·9
x/c

FIGURE - 7

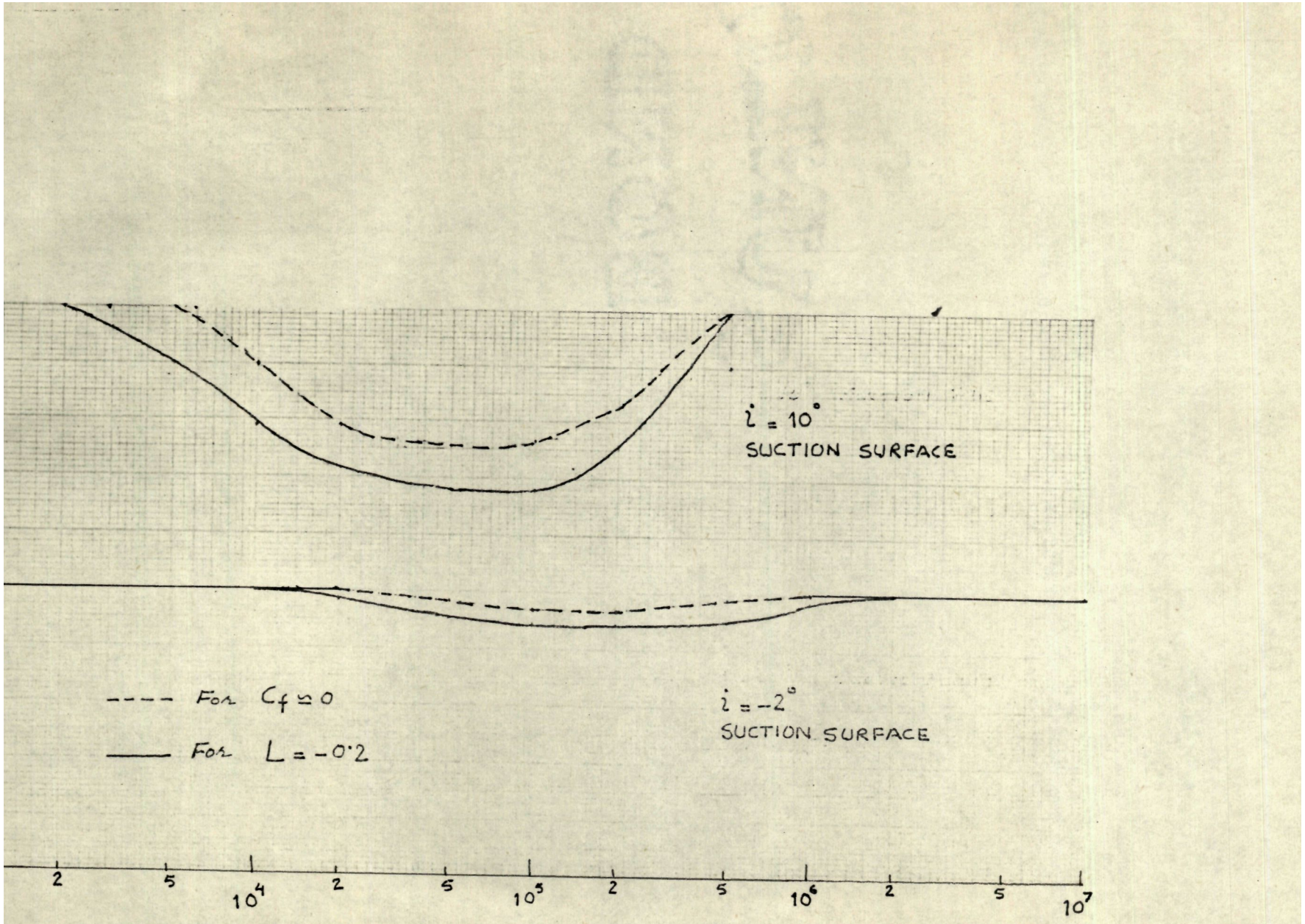
i = 10°
SUCTION SURFACE
---- For $C_f \simeq 0$
—— For $L = -0.2$
i = -2°
SUCTION SURFACE
2
5
$10^4$
2
5
$10^5$
2
5
$10^6$
2
5
$10^7$
BODY REYNOLDS NUMBER

FIGURE - 8

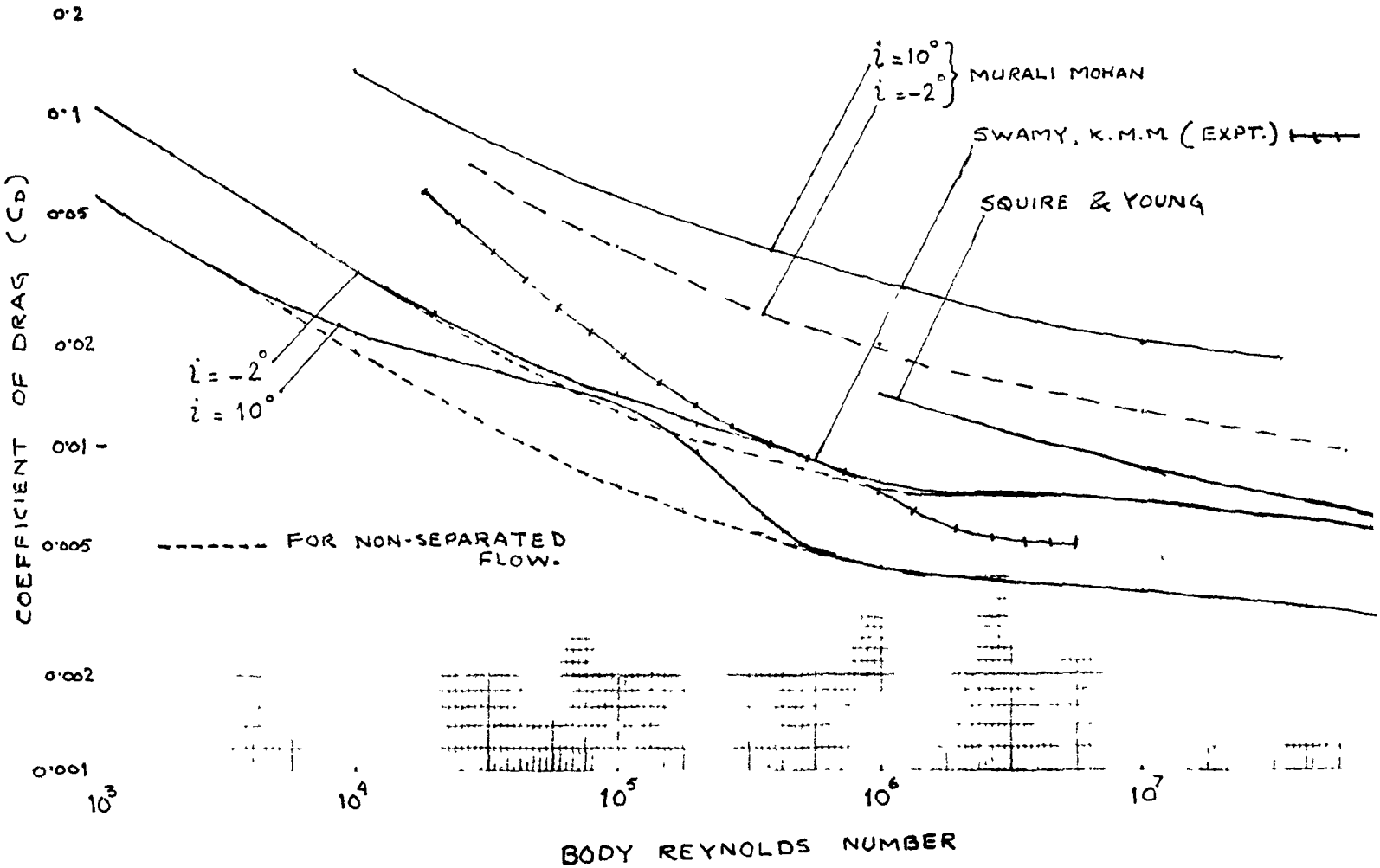
0·2
0·1
0·05
0·02
0·01
0·005
0·002
0·001
COEFFICIENT OF DRAG (CD)
i = 10°
i = -2°
MURALI MOHAN
SWAMY, K.M.M (EXPT.)
SQUIRE & YOUNG
i = -2°
i = 10°
------ FOR NON-SEPARATED FLOW.
10³
10⁴
10⁵
10⁶
10⁷
BODY REYNOLDS NUMBER

FIGURE - 9

```
      DO 3 I=1,M
      IF(XINT-X(I))5,1,2
1     YINT=Y(I)
      GO TO 7
2     IF(I-M)4,3,7
3     I=M-1
      GO TO 5
4     IF(XINT-X(I+1))5,1,1
5     YINT=(Y(I+1)-Y(I))/(X(I+1)-X(I))*(XINT-X(I))+Y(I)
      GO TO 7
6     CONTINUE
7     RETURN
      END
// FOR
      SUBROUTINE SPCON(X,Y,M,C)
      DIMENSION X(20),Y(20),D(20),P(20),E(20),C(4,20),A(20,3),B(20),Z(20
     N)
C     B.C.  SECOND DERIVATIVES AT THE ENDS POINTS ARE ZERO
C     SOLUTION OF SIMULTANEOUS EQNS. BY ELIMINATION METHOD
      MM=M-1
      Z(1)=0.&        Z(M)=0.
      DO 2 K=1,MM&        D(K)=X(K+1)-X(K)&        P(K)=D(K)/6.
2     E(K)=(Y(K+1)-Y(K))/D(K)
      DO 3 K=2,MM&3       B(K)=E(K)-E(K-1)
      A(2,2)=P(2)/(2.*(P(1)+P(2)))&        B(2)=B(2)/(2.*(P(1)+P(2)))
      A(2,3)=0.
      DO 4 K=3,MM&        A(K,2)=2.*(P(K-1)+P(K))-P(K-1)*A(K-1,3)
      B(K)=B(K)-P(K-1)*B(K-1)&        A(K,3)=P(K)/A(K,2)
    4 B(K)=B(K)/A(K,2)&        Z(MM)=B(MM)
      MN=M-2&        DO 6 I=2,MN&        K=M-I
6     Z(K)=B(K)-A(K,3)*Z(K+1)
      DO 7 K=1,MM&        Q=1./(6.*D(K))&        C(1,K)=Z(K)*Q
      C(2,K)=Z(K+1)*Q&        C(3,K)=Y(K)/D(K)-Z(K)*P(K)
      C(4,K)=Y(K+1)/D(K)-Z(K+1)*P(K)&7      CONTINUE&        RETURN
      END
// FOR
      SUBROUTINE SPLIN(X,Y,M,C,XINT,YINT,DY)
      DIMENSION X(20),Y(20),C(4,20)
C     CUBIC SPLINE IS USED
      IF(XINT)7,1,2&    1 YINT=Y(1)
      DY= (3.*C(1,1)*(X(2)-XINT)**2)+(3.*C(2,1)*(XINT-X(1))**2)-C(3,1)+C
     N(4,1)
       RETURN
    2 K=1&    3 IF(XINT-X(K+1))6,4,5&    4 YINT=Y(K+1)
      DY=-(3.*C(1,K)*(X(K+1)-XINT)**2)+(3.*C(2,K)*(XINT-X(K))**2)-C(3,K)
     N+C(4,K)
      RETURN
    5 K=K+1&        IF(M-K)7,7,3&    6 YINT=(X(K+1)-XINT)*(C(1,K)*(X(K+1)-
     NXINT)**2+C(3,K))+(XINT-X(K))*(C(2,K)*(XINT-X(K))**2+C(4,K))
      DY= (3.*C(1,K)*(X(K+1)-XINT)**2)+(3.*C(2,K)*(XINT-X(K))**2)-C(3,K)
     N+C(4,K)
      RETURN&    7 WRITE(5,101)
  101 FORMAT(20X,'OUT  OF  RANGE  FOR  INTERPOLATION')
      CALL EXIT
      END
// FOR
      DIMENSION XCSS(20),XCSP(20)
```

```
      M457,.0405,.0337,.0254,.016,.0106,0./
       DATA YY/3.1,2.4,2.0,1.8,1.6,1.5,1.4,1.35,1.3/
       DATAXX/-0.2,-0.18,-0.16,-0.13,-0.085, 0.05,0.,0.05,0.1/
       DATAAA/.5,.292893219,1.70710678,.1666666667/
       DATABB/2.,1.,1.,2./
       DATACC/.5,.292893219,1.70710678,.5/
       MM=9
       NA=17
       N=20
       AN=5.%       AM=4.%       A=0.0076
       SC=0.75
       STEP=0.005
        ALT=0.
       PI=4.*ATAN(1.0)
       PI1=PI/180.
        NXC=1./STEP
       NXC=NXC+1
       AL1=PI1*62.%       AL2=PI1*29.75%       ALM=PI1*50.8
       READ(8,108)(R(J),J=1,16)
       READ(8,100)(X(J),J=1,N)
       READ(8,100)(Y(J),J=1,N)
       DO 1 I=1,N%1      X(I)=X(I)/1.016
       CALL SPCON(XDA,YDA,NA,CA)
       WRITE(5,106)
       DO 38 L=1,4
       WRITE(5,101)
       CALL SPCON(X,Y,N,C)
       UU(1)=0
       SUM=0
       DO 9 I=2,NXC
       IF(L-2)7,2,4
2      IF(I-82)7,7,3
3      UU(I)=UU(82)
       GO TO 8
4      IF(L-4)7,5,39
5      IF(I-156)7,7,6
6      UU(I)=UU(156)
       GO TO 8
7      XC=(I-2)*STEP
       CALL SPLIN(X,Y,N,C,XC,CP,DY)
       UU(I)=COS(ALM)/COS(AL1)*SQRT(1.-CP)
C------------------------------------------------------------------
C    LAMINAR  BOUNDARY  LAYER  CALCULATIONS  BY  THWAITES  METHOD
8      SUM=SUM+(UU(I)**5+UU(I-1)**5)
       THER(I)=SQRT(0.45/(UU(I)**6)*(SUM-UU(2)**5)*STEP/2.)
9      CONTINUE
C------------------------------------------------------------------
C    DETERMINATION OF  TRANSITION  POINT  USING  MICHEL  CRITERION
       DO30J=1,16
       QS=0.
        S=R(J)
       AC=A/S**(1./6.)
       DO 12 I=2,NXC
       XC=(I-2)*STEP
       THE=THER(I)/SQRT(R(J))
       RX(I)=2.9*(UU(I)*XC*R(J))**0.4
```

```
15      II=I$          THET=THER(I)/SQRT(R(J))
        UUT=UU(I)
16      CONTINUE
C -------- ---------- ----------------------------------------
C    TURBULENT  BOUNDARY  LAYER  CALCULATIONS  BY  TRUCKENBRODT  METHOD
        C1=(THET*UUT**((3.*AN+3.)/(AN+1.)))**((AN+1.)/AN)
        SUM=0.$          SB=0.
        AX=0.$         AZ=0.
        DO 25 I=II,NXC
        IF(I-II)17,17,18
17      GO TO 19
18      SUM=SUM+(UU(I-1)**(3.+2./AN)+UU(I)**(3.+2./AN))
19      CONTINUE
        THE=(C1+A*SJM*STEP/2.0/S**(1./AN))**(AN/(AN+1.))/UU(I)**((3.*AN+3.
       B)/(AN+1.))
        RTHE(I)=UU(I)*THE*S
        XI(I)=(THE*UU(I)**((3.*AN+3.)/(AN+1.)))**(AM*((AN+1.)/AN))
        B(I)=0.07*ALOG(RTHE(I))/2.3 0.23
        IF(I II)24,24,20
20      CONTINUE
        ZZ=(THE*UU(I)**3)**(7./6.)
        DO 21 ITER=1,4
        AY=(B(I) ALOG(UU(I)/UUT))*4.*ZZ**3*AC*UU(I)**(10./3.)
        HK=(AY-BB(ITER)*AZ)*AA(ITER)
        AZ=AZ+3*HK-CC(ITER)*AY
        AX=AX+HK*STEP
21      CONTINUE
        AL=ALOG(UU(I)/UUT)+AX/XI(I)
        CALL INTPL(XX,YY,MM,AL,H)
        CF=0.246/10.0**(0.678*H)/RTHE(I)**0.268
        IF(QS)24,22,24
22      IF(CF-0.0001)39,39,36
C  22 IF(AL+0.20)39,39,36
23      XINT=(I-2)*STEP
        CALL SPLIN(XDA,YDA,NA,CA,XINT,YINT,DY)
        QS=YINT*((UU(I)/UU(202))**2-.9)/2.
24      CONTINUE
25      CONTINUE
26      IF(L-2)28,29,27
27      IF(L-4)28,29,39
28      THS(J)=THE
        TH(J)=QS
        XCSS(J)=XINT
        XCTS(J)=XC
        GO TO 30
29      THP(J)=THE
        THH(J)=QS
        XCSP(J)=XINT
        XCTP(J)=XC
30      CONTINUE
        IF(L-2)34,32,31
31      IF(L-4)37,32,39
32      CONTINUE
        DO 33 J=1,16
        HH=(THS(J)+THP(J)+TH(J)+THH(J))/(SC*COS(AL2))
        CD=2.*SC*HH*(COS(ALM))**3/(COS(AL2))**2
```

```
      READ(8,100)(Y(J),J=1,N)
      DO 35 I=1,N&35     X(I)=X(I)/0.984
      GO TO 38
36    N=20
      READ(8,100)(X(J),J=1,N)
      READ(8,100)(Y(J),J=1,N)
      WRITE(5,107)
      AL1=PI1*50.
       AL2=PI1*26.5
      ALM=PI1*40.2
      GO TO 38
37    READ(8,100)(X(J),J=1,N)
      READ(8,100)(Y(J),J=1,N)
38    CONTINUE
39    CALL EXIT
 100  FORMAT(8F10.3)
101   FORMAT(20X,'----------                    ')
106   FORMAT(//20X,' I N C I D E N C E = 10  D E G ')
107   FORMAT(//20X,' I N C I D E N C E = -2  D E G ')
108   FORMAT(8E10.3)
109   FORMAT(1X,E7.1,4F7.3,4E11.3,2E12.4)
       END
 0.100E 04 0.200E 04 0.500E 04 0.100E 05 0.200E 05 0.500E 05 0.100E 06 0.200E 0
 0.500E 06 0.100E 07 0.200E 07 0.500E 07 0.100E 08 0.200E 08 0.500E 08 0.100E 0
0.          0.026     0.041     0.045     0.066     0.116     0.166     0.216
0.266       0.316     0.366     0.416     0.666     0.716     0.766     0.816
0.866       0.916     0.966     1.016
1.         -1.74     -1.78     -1.74     -1.57     -1.05     -0.81     -0.65
-0.5025    -0.42     -0.325    -0.24      0.115     0.19      0.23      0.28
0.31        0.325     0.35      0.36
0.          0.009     0.034     0.059     0.084     0.134     0.184     0.234
0.384       0.484     0.534     0.584     0.734     0.784     0.834     0.834
0.934       0.984
1.          0.88      0.65      0.5       0.47      0.475     0.475     0.47
0.475       0.485     0.505     0.51      0.51      0.505     0.49      0.475
0.45        0.425
0.0         0.025     0.05      0.1       0.15      0.2       0.25      0.3
0.4         0.5       0.55      0.6       0.65      0.7       0.75      0.8
0.85        0.9       0.95      1.0
1.0        -0.45     -0.7      -0.66     -0.64     -0.625    -0.62     -0.59
-0.5       -0.42     -0.36     -0.31     -0.235    -0.1505   -0.08      0.01
0.1         0.19      0.29      0.365
0.0         0.016     0.0375    0.0506    0.1167    0.15      0.2       0.25
0.3         0.35      0.45      0.5       0.55      0.65      0.7       0.8
0.85        0.9       0.95      1.0
1.0         0.2      -0.08      0.1       0.0       0.05      0.125     0.175
0.215       0.25      0.32      0.34      0.36      0.39      0.4       0.405
0.4         0.39      0.37      0.34
```